Nature Communications

https://doi.org/10.1038/s41467-026-72165-6

Article in Press

Activating p53^{Y220C} with a mutant-specific small molecule

Received: 5 December 2025

Accepted: 7 April 2026

Cite this article as: Zhu, X., Byun, W.S., Pieńkowska, D.E. *et al.* Activating p53^{Y220C} with a mutant-specific small molecule. *Nat Commun* (2026). https://doi.org/10.1038/s41467-026-72165-6

Xijun Zhu, Woong Sub Byun, Dominika Ewa Pieńkowska, Kha The Nguyen, Mengxiong Wang, Sabin A. Nettles, Sai Gourisankar, Nick A. Phillips, Jan Gerhartz, Qixiang Geng, Tian Qiu, Jianing Zhong, Zixuan Jiang, Roman C. Sarott, Stephen M. Hinshaw, Tinghu Zhang, Laura D. Attardi, Radosław P. Nowak & Nathanael S. Gray

Activating p53^{Y220C} with a Mutant-Specific Small Molecule

Xijun Zhu[1#], Woong Sub Byun[2,3#], Dominika Ewa Pieńkowska[4#], Kha The Nguyen[5,6], Mengxiong Wang[5,6], Sabin A. Nettles[7], Sai Gourisankar[2], Nick A. Phillips[8], Jan Gerhartz[4], Qixiang Geng[2], Tian Qiu[2], Jianing Zhong[1], Zixuan Jiang[1], Roman C. Sarott[2], Stephen M. Hinshaw[2], Tinghu Zhang[2], Laura D. Attardi[5,6,8*], Radosław P. Nowak[4*], Nathanael S. Gray[2*]

[1]Department of Chemistry, Stanford University, Stanford, CA, USA.
[2]Department of Chemical and Systems Biology, ChEM-H, Stanford Cancer Institute, School of Medicine, Stanford University, Stanford, CA, USA.
[3]College of Pharmacy, Dongguk University-Seoul, Goyang 10326, Republic of Korea
[4]Institute of Structural Biology, Medical Faculty, University of Bonn, Bonn, Germany
[5]Division of Radiation and Cancer Biology, Department of Radiation Oncology, Stanford University School of Medicine, Stanford, CA, USA.
[6]Department of Genetics, Stanford University School of Medicine, Stanford, CA, USA.
[7]Department of Pathology, Stanford University School of Medicine, Stanford, CA, USA
[8]Cancer Biology Program, Stanford School of Medicine, Stanford University, Stanford, CA, USA.

[#]These authors contributed equally to this work.
*Correspondence to: nsgray01@stanford.edu; radoslaw.nowak@uni-bonn.de; attardi@stanford.edu

ABSTRACT

TP53 is the most commonly mutated gene in cancer, but it remains recalcitrant to clinically meaningful therapeutic reactivation. We present here the discovery and characterization of a small molecule chemical inducer of proximity that activates mutant p53. We named this compound TRanscriptional Activator of p53 (**TRAP-1**) due to its ability to engage p53^{Y220C} and BRD4 in a ternary complex, which potently activates mutant p53 and triggers robust p53 target gene transcription. Treatment of p53^{Y220C}-expressing cell lines with **TRAP-1** results in rapid upregulation of *CDKN1A* and other p53 target genes and induces cellular senescence and apoptosis. Negative control compounds that are unable to form a ternary complex lack these activities,

demonstrating the necessity of chemically induced proximity for the observed pharmacology. This approach to activating mutant p53 highlights how chemically induced proximity can be used to restore the functions of tumor suppressor proteins that have been inactivated by mutation in cancer.

INTRODUCTION

The p53 protein is a transcription factor that activates multiple antiproliferative signaling pathways, including cell cycle arrest and apoptosis, in response to DNA damage, ribosomal stress, and oncogenic signaling[1,2]. In the absence of these stresses, the ubiquitin ligase Mouse double minute 2 homolog (MDM2) keeps p53 protein levels low[1]. When this negative regulation is released, p53 activates anti-neoplastic programs, such as cell cycle arrest, senescence, apoptosis, and differentiation[3]. Due to these functions, *TP53* is the most commonly mutated gene found in cancer, with ~50% of patients showing somatic mutations across a range of tumor types[4]. Approximately 80% of sequenced p53 lesions are missense mutations that cluster in the DNA-binding domain[5,6]. These mutations cause reduced thermal stability and/or impaired DNA binding, thus compromising the tumor suppressor function[7].

For decades, restoring p53 function has been a goal in the development of cancer therapeutics. These efforts have stimulated the development of MDM2 inhibitors, such as nutlin-3a, which lead to stabilization of $p53^{WT}$ [8] (Fig. 1A). Severe thrombocytopenia limits the therapeutic use of nutlin-3a and related molecules[9,10]. Another approach to restoring p53 function is to stabilize the mutated protein with directed small molecule ligands. Recently, several groups have developed a series of small molecule p53 "correctors" that increase the thermal stability and partially restore the transcriptional activity of mutated p53[11]. These p53 corrector molecules target a structural cavity created by $p53^{Y220C}$ [12], a hotspot mutation affecting ~120,000 patients per year and accounting for approximately 1.6% of p53 missense mutations[4,6,13,14]. Several successful medicinal chemistry campaigns have targeted the $p53^{Y220C}$ pocket to improve the thermal stability of mutant p53 (Fig. 1A). An initial *in silico* screen followed by structural investigation identified a carbazole fragment PhiKan083 with weak binding affinity to $p53^{Y220C}$ [15]. Further optimization of this scaffold produced the lead compounds PK5196 and PK9328 with enhanced binding affinity, leading to increased expression of p53 target genes and improved antiproliferative activity in cells[16,17]. Using a similar approach, PMV Pharmaceuticals and Jacobio Pharmaceuticals have developed the mutant-specific small molecule p53 binders rezatapopt (PC14586) and JAB-30355[18-21], respectively. In addition, the presence of a reactive cysteine in the $p53^{Y220C}$ inspired the synthesis of covalent-acting fragments such as KG13, which selectively targets mutant p53 via covalent modification of the sulfhydryl group of the cysteine 220 side chain using a methyl acrylamide

warhead[22]. Despite these advances, it is not clear to what extent partial $p53^{Y220C}$ functional restoration will provoke a clinically meaningful outcome. A major unresolved question is whether enhancing the thermal stability of mutant p53 to wild-type (WT) levels is sufficient for cancer therapy, or if further activation is also required. Small molecule p53 activators are required to answer this question.

The advent of event-driven pharmacology, enabled by chemically induced proximity, has expanded the scope of targets addressable by small molecules. Leveraging molecular proximity as a unifying regulatory principle, small molecules that induce new protein-protein interactions have enabled precise control over cellular signaling, including rewiring of protein degradation pathways[23,24]. These strategies offer major advantages beyond traditional occupancy-based pharmacology: *i*) a single small molecule may catalyze multiple rounds of degradation, transcription, etc., *ii*) efficacy does not require complete target occupancy, and *iii*) the use of dual targets creates a logical "AND" gate, resulting in enhanced cellular and biochemical selectivity. Recently reported p53-targeting small molecules that purport to take advantage of these characteristics include those that induce mutant p53 degradation[25], p53 acetylation[26-28], p53 stabilization by deubiquitylation[29,30], and selective mutant p53 cancer cell killing by inducing p53-dependent toxicity[31]. Here we seek to leverage the induced proximity strategy to directly restore the core function of mutant p53: transcriptional activity.

To activate p53, we took inspiration from an approach we have recently developed that uses small molecules to reprogram transcription factors. These small molecules, which are called transcriptional/epigenetic chemical inducers of proximity (TCIPs), recruit transcriptional coactivators (BRD4 or CDK9/pTEF-B) to gene promoters bound by the transcriptional repressor protein, BCL6 (B cell lymphoma 6)[32,33] . Treatment of BCL6-high B cell lymphomas with TCIPs rapidly activates a suite of cell death genes normally repressed by BCL6, resulting in tumor cell-specific cell death. Here we apply this logic to develop mutant-specific small molecules TRanscriptional Activators of p53 (TRAPs). We report proof-of-concept TRAPs that recruit the transcriptional coactivator protein BRD4 to $p53^{Y220C}$. These small molecules activate p53 and produce enhanced pharmacology when compared with existing small molecules that can only

restore p53 thermal stability. Further development of TRAPs towards clinical candidates has the potential to provide clinical benefit to patients with $p53^{Y220C}$ cancers.

RESULTS

Small molecules that specifically activate a p53 mutant

To enable discovery of p53 activator compounds, we developed a p53 luciferase reporter assay in $p53^{Y220C}$ bearing BxPC-3 cells[34], which consists of two copies of a p53 response element (p53 RE) that drives the transcription of the luciferase reporter gene. We first used this assay to search for small molecule p53 binders that could serve as starting points for bivalent compound synthesis. We screened a series of published $p53^{Y220C}$ correctors[17,19,22], the MDM2 inhibitor nutlin-3a[8], and the acetylation targeting chimera (AceTAC) molecule MS78 that induces p53 acetylation[27]. Among these, the B-1 binder[19], which shares the same chemotype as the currently reported $p53^{Y220C}$ selective clinical candidates[20], was the only compound that showed a modest response (Supplementary Fig. 1A and 1B). Based on these results, we next synthesized a tool compound, **B-1 linker** (Supplementary Fig. 1B), where the methyl piperidine in B-1 was functionalized with a short alkyl linker through amide bond coupling[35]. **B-1 linker** produced enhanced transcriptional activation in the reporter assay relative to the parental B-1 molecule (Supplementary Fig. 1A). We characterized $p53^{Y220C}$ binding to **B-1 linker** using nano-differential scanning fluorimetry (NanoDSF). In this assay, $p53^{Y220C}$ is less stable than its wild-type counterpart ($p53^{Y220C}$ – T_m 33.90°C ± 0.44°C; $p53^{WT}$ – T_m 41.11°C ± 0.08°C). **B-1 linker** stabilized $p53^{Y220C}$ with ΔT_m 6.33°C ± 0.61°C versus DMSO, whereas B-1 produced more modest stabilization at ΔT_m 4.55 ± 0.10°C (Supplementary Fig. 1C). This suggests that functionalization of B-1 with a linker did not impede p53 binding and possibly contributed additional favorable protein-ligand interactions, aiding in the restoration of p53 function.

Knowing that presence of a linker did not affect the functional response, we used **B-1 linker** as the basis for a library of small molecules where the B-1 binder was linked to the bromodomain ligand JQ1[36] through alkyl, PEG, and rigid diamine linkers (Fig. 2A). JQ1 recruits BRD4 without inhibiting its transcriptional activator function[32,37-39]. We next asked if the compounds in the library can induce a complex between BRD4 and $p53^{Y220C}$ *in vitro*. To test this, we used recombinant $p53^{Y220C}$ DNA binding domain to establish a time-resolved fluorescent energy

transfer (TR-FRET) assay between $BRD4_{BD1}$ and $p53^{Y220C}$ (Fig. 2B). Due to the bifunctional nature of the molecules, we expected to observe a reduction of complex formation when excess bivalent molecules saturate individual protein binding sites rather than forming the ternary complex, a phenomenon commonly called the "hook effect"[40]. Among the tested compounds, those with methylene-connected (**462**, **463**) or spiro (**464**) six-membered heterocycle linkers showed bell-shaped curves, with the greatest TR-FRET ratios at the peak and a visible "hook effect" (Fig. 2B), while compounds with smaller rigid linkers, flexible alkyl, and PEG linkers produced much weaker signals (Supplementary Fig. 1D). Additionally, minor structural changes in the linkers, such as removing the methylene spacer (**537**) or replacing one nitrogen atom on the six-membered ring (**540**), resulted in a rightward shift of the curve (Supplementary Fig. 1D). Taken together, the biochemical data identified compounds **462** (**TRAP-1**), **463** (**TRAP-2**), and **464** (**TRAP-3**) as small molecules that induce proximity between the $p53^{Y220C}$ DNA binding domain and $BRD4_{BD1}$.

Using the p53 reporter assay, we proceeded to screen our compound library to assess p53-dependent transcriptional activity. We compared these results with co-treatment of cells with the individual binders as a control. JQ1 did not induce p53 target gene activation at concentrations up to 10 μM (Supplementary Fig. 1A). Co-treatment with **B-1 linker** and JQ1 produced modest reporter activation (12-fold versus DMSO) compared with the **B-1 linker** alone (Fig. 2C and Supplementary Fig. 1A). In contrast, **TRAP-1**, **TRAP-2**, and **TRAP-3** each produced dose-dependent reporter activation, with **TRAP-1** inducing 40-fold target gene transcription upregulation versus DMSO at 10 μM concentration (Fig. 2C). Further increasing the concentration beyond 10 μM resulted in a decrease in luciferase signal (Fig. 2C), recapitulating the "hook effect" observed in the TR-FRET dimerization assay. Compounds that showed lower dimerization ability in the TR-FRET assay induced lower or no transcription activation at the concentration range tested (Supplementary Fig. 1E). This observation, along with a strong overall correlation between reporter gene induction and biochemical binding as measured by TR-FRET (Supplementary Fig. 1F), suggests that transcriptional activation of p53-dependent transcription depends on chemically induced BRD4-p53 proximity. Collectively, the data suggest that **TRAP-1**, **TRAP-2**, and **TRAP-3** are potent $p53^{Y220C}$ transcriptional activators.

We next sought to explore compounds featuring different $p53^{Y220C}$ selective binders. For this, we focused on PK9328[17] as the $p53^{Y220C}$ binder because it has been previously used for the development of MS78, an acetylation-inducing chimera[27] (Supplementary Fig. 2A). Treatment with the free amine form of PK9328 alone did not produce transcriptional activation in the reporter assay (Supplementary Fig. 1A), and the synthesis of a similar small library of TRAP candidate compounds produced no active compounds in the TR-FRET dimerization (Supplementary Fig. 2B) or luciferase reporter assays (Supplementary Fig. 2C).

Transcriptional activation requires ternary complex formation

To test whether transcriptional activation by our molecules depends on co-binding to $p53^{Y220C}$ and BRD4, we designed and synthesized negative control compounds with minor chemical modifications that disrupt binding to either BRD4 (**TRAP-1-NegB**) or $p53^{Y220C}$ (**TRAP-1-NegP**). Using **TRAP-1** as a template (Fig. 3A), **TRAP-1-NegB** was synthesized with an opposite chiral configuration to reduce BRD4 binding[36]. Likewise, **TRAP-1-NegP** was designed with two extra methylations on the B-1 nitrogen atoms to remove the H-bond interactions that were shown to be crucial for $p53^{Y220C}$ binding[20,21,41]. **TRAP-1** and **TRAP-1-NegB** stabilized $p53^{Y220C}$ to a similar degree in NanoDSF experiments, while **TRAP-1-NegP** did not have this activity (**Fig. 3B** and Supplementary Fig. 3A). Compared with the lead compounds, the negative controls showed negligible ternary complex formation in the TR-FRET dimerization assay (Fig. 3C) and no transcriptional activation in the reporter assay (Fig. 3D). Additionally, a TR-FRET assay between $p53^{WT}$ and BRD4 resulted in no TRAP-induced ternary complex (Supplementary Fig. 3B). These data confirm direct binding of **TRAP-1** to $p53^{Y220C}$ and that the enhanced transcriptional activation is associated with the ternary complex formation between $p53^{Y220C}$, BRD4, and the compound. Furthermore, the observed chemically induced proximity is p53 mutant-specific.

To assess the cooperativity of the TRAP-induced ternary complex, we established a $p53^{Y220C}$ TR-FRET binding assay based on displacement of a $p53^{Y220C}$ binding FITC-tracer probe. The negative control compound **TRAP-1-NegP** did not bind to $p53^{Y220C}$, confirming the specificity of the observed interaction. Inclusion of BRD4 in these experiments enhanced **TRAP-1**-$p53^{Y220C}$ binding, indicative of cooperative ternary complex formation (α = 1.2; Supplementary Fig. 3C).

We then performed co-immunoprecipitation experiments to test the idea that TRAPs induce $p53^{Y220C}$-BRD4 binding in cells. HEK293T cells were transfected with plasmids coding for FLAG-BRD4 and $p53^{Y220C}$-V5, and anti-FLAG beads were used to isolate BRD4-associated proteins from cell lysates after cellular compound treatment. $p53^{Y220C}$ pulled down with BRD4 after cell treatment with TRAPs; **TRAP-1** and **TRAP-2** induced stronger interactions than **TRAP-3** (Fig. 3E). Co-treatment with the two parental compounds did not induce an interaction (Fig. 3E). Taken together, these data demonstrate that TRAPs induce a stable interaction between $p53^{Y220C}$ and BRD4 in cells.

TRAP-1 activates p53 target genes

We next evaluated the immediate transcriptional consequences of treatment with TRAPs. To this end, we examined validated direct transcriptional targets of p53 with known functions in p53 regulation (*MDM2*), cell cycle arrest (*CDKN1A*), and apoptosis (*PMAIP1*, *BBC3*, and *BAX)*[17,18,22]. We used reverse transcription quantitative PCR (RT-qPCR) to measure mRNA levels in BxPC-3 cells. Time course experiments after treatment with 3 μM of **TRAP-1** showed time-dependent upregulation of *MDM2* and *CDKN1A* as early as 2 h after incubation, with maximum levels accumulating at approximately 8 h post-treatment (Supplementary Fig. 4A). The apoptosis-effector genes *PMAIP1* and *BBC3* showed modest mRNA increases. *TP53* mRNA levels were not affected by the molecules (Supplementary Fig. 4A). To compare TRAPs with the parental compounds, we measured p53 target gene levels by RT-qPCR after 8 h of treatment. We tested **TRAP-1**, the parental binders, and the two negative controls in BxPC-3 cells. **TRAP-1** induced mRNA expression for *MDM2* (6.1-fold versus DMSO), *CDKN1A* (169-fold versus DMSO), and *BBC3* (9.8-fold versus DMSO), with *CDKN1A* showing the greatest response among all genes being evaluated (Fig. 4A). Induction was stronger for **TRAP-1** than for B-1, JQ1, or **TRAP-1-NegB** and **TRAP-1-NegP**. In the case of *CDKN1A*, **TRAP-1** treatment induces over 25-fold more transcripts than other treatments (Fig. 4A; 169-fold for **TRAP-1** /6.6-fold for JQ1). These data match the results from reporter gene assays and the kinetics of gene activation we have observed for the best TCIP compounds[32,42]. Overall, these results indicate that TRAPs induce robust expression of direct p53 target genes, likely by recruiting BRD4 to the sites bound by chemically corrected $p53^{Y220C}$.

To further investigate the global gene regulation specifically induced by **TRAP-1**, we performed RNA sequencing on BxPC-3 cells treated with 3 μM of **TRAP-1** or controls at both 2 h and 4 h timepoints. Principal component analysis of gene counts revealed strong clustering of replicates and separation between treatment groups (Supplementary Fig. 4B). We then performed differential expression analysis and gene set enrichment analysis (GSEA) for each treatment versus DMSO. We observed stronger enrichment of hallmark p53 pathway gene set from the Molecular Signature Database (MSigDB) in the **TRAP-1** treated cells at both the 2 h and 4 h timepoints compared with control treated cells (Fig. 4B). We then examined a list of the top 116 p53 target genes identified from a meta-analysis of genome-wide datasets as consistently induced in numerous human cell lines[43]. We assessed the induction of these genes at the 4 h time point and observed significantly increased expression for 71.1% of these target genes for **TRAP-1**, compared to 57.0% for JQ1, 53.1% for **TRAP-1-NegP**, 22.8% for MS78, and 5.3% for **TRAP-1-NegB** (Fig. 4C and Supplementary Fig. 4C). Furthermore, differential expression analysis and gene set enrichment analysis of p53 pathway genes in **TRAP-1** revealed significant enrichment relative to JQ1 (normalized enrichment score = 2.01, adjusted p value = $2.9*10^{-9}$) and **TRAP-1-NegP** (normalized enrichment score = 2.1, adjusted p value = $10*10^{-12}$). Overall, these results underscore the ability of **TRAP-1** to induce p53-activated genes, reinforcing its role as a selective modulator of the p53 pathway.

We next used Western blotting to evaluate whether elevated mRNA levels for p53 target genes correspond to elevated protein expression. Treatment with **TRAP-1**, **TRAP-2**, and **TRAP-3** for 16 h in BxPC-3 cells caused robust upregulation of p21 (encoded by *CDKN1A*) and MDM2 protein levels (Fig. 4D). The parental binders did not have this effect. We observed no significant changes in p53, PUMA (encoded by *BBC3*), or BAX protein levels at this time point for any of the tested compounds. Potent upregulation of p21 was evident as early as 2 h after treatment with **TRAP-1**, highlighting the rapid and likely direct effect of the small molecules on p53 target genes (Fig. 4E).

Induction of cell cycle arrest factors, and p21 in particular, suggests that TRAPs may irreversibly reprogram cancer cell transcription. To test the idea that a pulsatile treatment with **TRAP-1** might be sufficient to trigger an inescapable growth arrest, we conducted a washout experiment. BxPC-3 cells were treated with **TRAP-1** for two hours – sufficient time to induce high levels of p21 protein

– and the small molecules were subsequently washed away. After this, we replated equal numbers of live cells for unperturbed proliferation for 72 h. **TRAP-1** inhibited cell proliferation in this assay, while the control **B-1 linker** did not (Fig. 5A). Moreover, strong p21 expression was detected 24 h after washout in **TRAP-1** treatment, but not in controls (Fig. 5B). Collectively, these data demonstrate that **TRAP-1** can induce rapid and potent transcriptional activation in cells, and the washout result suggests that the effect can persist even after the compounds are removed.

To further understand the antiproliferative ability of **TRAP-1** in BxPC-3 cells, we evaluated cell cycle progression by measuring BrdU incorporation during DNA replication. BrdU was added to BxPC-3 cell cultures for the final 4 h of a 24 h compound treatment. **TRAP-1** (3 μM) prevented BrdU incorporation, whereas neither the negative controls nor MS78 had this effect (Fig. 5C and Fig. 5D). Thus, **TRAP-1** stalls cell cycle progression via a mechanism not shared with either BRD4 (**TRAP-1-NegP**) or $p53^{Y220C}$ (**TRAP-1-NegB**) binding controls.

We next sought to investigate the fate of the arrested cells at later timepoints. In A549 p53-knockout cells complemented with *TP53-Y220C* (A549-$p53^{Y220C}$ cells), a 6-day treatment with **TRAP-1** (3 μM) yielded few remaining cells, with strong senescence-associated (SA)-β-gal staining observed in most of the survivors. Senescent cell staining was generally absent from control treatments, and JQ1 produced relatively few senescent cells (Fig. 5E and Fig. 5F). We next assessed the apoptosis-promoting activity of **TRAP-1** using annexin V-FITC/propidium iodide staining in cells. **TRAP-1** induced apoptosis in over 40% of the cell population while JQ1 induced slightly less apoptosis, and the negative controls induced relatively little apoptosis (Fig. 5G and Supplementary Fig. 5). Crucially, all compounds were used at 3 μM in this experiment, resulting in roughly 180-fold greater BRD4 occupancy by JQ1 versus **TRAP-1** and its controls as judged by NanoBRET BRD4 cellular engagement (Supplementary Fig. 6A**;** EC_{50} 4.0 μM/0.022 μM). Collectively, these data indicate that **TRAP-1** selectively triggers cellular senescence and apoptosis.

TRAP-1 activity is p53 mutant-specific

Having explored the potential of the p53 transcriptional activator to induce cellular senescence and apoptosis, we next investigated the antiproliferative effects of the compounds across a panel of

cell lines with different p53 mutational statuses. Based on the biochemical p53 mutant selectivity of the TRAPs in the TR-FRET dimerization assay (Supplementary Fig. 3B), we compared the cell viability among BxPC-3 cells ($p53^{Y220C}$), A549 cells ($p53^{WT}$), and a non-tumorigenic colon epithelial cell line CCD 841 CoN ($p53^{WT}$). Treatment with **TRAP-1**, **TRAP-2**, and **TRAP-3** for 72 h exhibited antiproliferative activity in BxPC-3 ($p53^{Y220C}$) cells with submicromolar IC_{50} values, while compounds that induce weaker or no p53-BRD4 proximity had a weaker antiproliferative effects (Fig. 6A). **TRAP-1** exhibited 7.4-fold more potent antiproliferative activity in BxPC-3 cells than in A549 cells after a 3-day treatment (Fig. 6B; IC_{50} 3.9 µM A549/0.53 µM BxPC-3) and 21-fold more potent activity than in CCD 841 CoN cells after a 5-day treatment (Fig. 6B; IC_{50} 6.5 µM CCD 841 CoN/0.31 µM BxPC-3). We also observed modest antiproliferative activity with **TRAP-1**, **TRAP-1-NegP**, and **TRAP-1-NegB** in A549 cells ($p53^{WT}$, Fig. 6B; IC_{50} 3.9 µM, 3.1 µM, and 7.5 µM). Although JQ1 showed similar antiproliferative potency as **TRAP-1**, JQ1 is roughly 180-fold more cell-penetrant than **TRAP-1** (Supplementary Fig. 6A; EC_{50} 4.0 µM/0.022 µM). The lower cellular effective concentration of **TRAP-1** indicates it has a higher per-molecule cytotoxic effect than its monovalent counterpart. To further confirm the antiproliferation selectivity of **TRAP-1** in isogenic cells with different p53 statuses, we knocked out *TP53* in A549 cells and then reintroduced $p53^{WT}$ or $p53^{Y220C}$ to generate A549-$p53^{-/-}$, A549-$p53^{WT}$, and A549-$p53^{Y220C}$ cell lines. The parental binders and binder co-treatment showed similar antiproliferative activities across the three cell lines, and **TRAP-1** was only modestly more potent ($p53^{Y220C}$ - IC_{50} 1.0 µM; $p53^{-/-}$ - IC_{50} 3.8 µM; $p53^{WT}$ - IC_{50} 3.5 µM; Supplementary Fig. 6B). **TRAP-1-NegB**, **TRAP-1-NegP**, and MS78 showed similar antiproliferative effects in all three isogenic cell lines, demonstrating a lack of selectivity for $p53^{Y220C}$ cells (Supplementary Fig. 6B). Likewise, p21 protein upregulation was unique to TRAP-1 treatment in A549-$p53^{Y220C}$ cells; it was not observed for other compounds or cell lines (Supplementary Fig. 6C). Taken together, these results suggest that **TRAP-1** induces a mutant-specific ternary complex that drives p21 upregulation and consequent cell cycle arrest and apoptosis.

DISCUSSION

Transcriptional dysregulation is a hallmark of cancer[44]. Overactivity of oncogenic transcription factors and loss of tumor suppressor transcription factors both enable cancer cells to escape normal control of cell proliferation[45]. While there have been successful approaches to inhibiting oncogenic

transcription factors[46], there have not yet been actionable medicinal chemistry design strategies for activating tumor suppressor transcription factors like p53. Proof of concept experiments carried out in mouse models of disease that demonstrate p53 reactivation as a viable cancer treatment strategy have been reviewed by Bieging et al.[47,48] Until now, direct chemical activators of mutant p53 have yet to deliver on the promise of this concept.

Here, we developed a small molecule approach to generate p53 transcriptional activators. To do this, we chemically fused the transcriptional co-activator function of BRD4 to the restored DNA binding activity of $p53^{Y220C}$. The resulting lead compound **TRAP-1** induced an interaction between $p53^{Y220C}$ and BRD4. The ternary complex was p53 mutant-specific and activated p53 target gene transcription rapidly, potently, and dose-dependently in $p53^{Y220C}$ bearing cells. The transcriptional activation was significantly stronger than that observed upon treatment with parental $p53^{Y220C}$ corrector, B-1, either given alone or in combination with the BRD4 binder JQ1. Treatment of **TRAP-1** selectively stalled cell cycle progression and induced cellular senescence, consistent with the tumor suppressive responses of p53 activation *in vivo* with a hyperactive p53 mutant[48].

Our experiments indicate that **TRAP-1** activates p53 by an induced proximity mechanism. Previous studies describe a synergistic relationship between BRD4 (with CPI203) and MDM2 inhibition (with nutlin-3). This was observed in acute myeloid leukemia cells[49]. Our biochemical and cellular data indicate that transcriptional activation induced by **TRAP-1** is fundamentally distinct at a mechanistic level. **TRAP-1** induced p21 and MDM2, produced a modest increase in apoptosis-related gene mRNAs, and displayed cellular senescence- and apoptosis-inducing activity in $p53^{Y220C}$ expressing cells. These and other activities correlated well with biochemical ternary complex and were obviated by minimal chemical modifications of **TRAP-1** to produce negative control compounds. Further efforts to find TRAP candidates using a different $p53^{Y220C}$ ligand, PK9328, which was inactive in our p53 reporter assay, failed to produce active compounds, suggesting the activities of **TRAP-1** are not simply due to inhibition of BRD4 and stabilization of p53 separately, but rather reflect formation of a specific ternary complex.

This work demonstrates an approach to activating p53 through the formation of a complex with BRD4 via chemically induced proximity. The ternary complex we report produces a gain-of-function mechanism that differs from recent ternary complex-dependent inhibition strategies. These include a bifunctional molecule (p53-01) that uses $p53^{Y220C}$ as a cellular anchor to enrich a linked PLK1 inhibitor, resulting in apoptosis that does not depend on p53 reactivation[31]. A second ternary complex-dependent mechanism involves localized BRD4 inhibition at c-MYC promoters via dCas9-mediated targeting[50]. Unlike these compelling inhibition-based mechanisms, the **TRAP-1** mechanism entails selective activation of mutant p53, leading to cell cycle arrest and apoptosis. Indeed, the **TRAP-1** mechanism resembles that of recent BCL6-activating small molecules (so-called "TCIPs")[32,33], despite the fact that the ternary complex dependence of antiproliferation activity we report here is numerically less impressive. A recent report of similar $p53^{Y220C}$-activating bivalent small molecules demonstrates the therapeutic potential of this mechanism[51].

Further optimization of **TRAP-1** is needed to enhance its potency and mitigate cell cytotoxicity from BRD4 inhibition. Efforts to use different effector proteins and tumor-specific factors are also currently underway. Besides BRD4, chromatin-modifying enzymes such as bromodomain and PHD finger containing 1 (BRPF1), histone acetyltransferase paralogues p300 and CREB-binding protein (CBP), and others have been recruited for endogenous gene activation[38,52]. Our group has also demonstrated the chemically induced proximity with transcriptional kinase CDK9 as a gain-of-function strategy to activate apoptosis[33]. In addition to these effectors, disease-specific driver proteins are potential candidates for the development of advanced TRAP molecules with improved selectivity and reduced on-target toxicity derived from effector occupancy.

Previous studies on bifunctional compounds that target p53 mainly focused on p53 post-translational modification[26-28], increasing p53 protein abundance[25,29], and cellular enrichment of toxic molecules[31]. **TRAP-1** embodies an approach to directly potentiate p53 transcriptional activity through protein-protein interaction induced by bivalent or monomeric molecular glue compounds. This strategy demonstrates the potential of chemically induced proximity to directly activate transcription factor function. While our study focuses on $p53^{Y220C}$ specifically, this

approach provides a potential solution to the challenge of developing activators for tumor suppressors that are dysregulated in cancer cells.

METHODS

Chemical Synthesis

Additional details are provided in the supporting information.

Cell Culture

Human pancreatic cancer (BxPC-3, ATCC, CRL-1687), kidney epithelial (HEK293T, ATCC, CRL-3216), lung cancer (A549, ATCC, CCL-185), and colon epithelial (CCD 841 CoN, ATCC, CRL-1790) cell lines were obtained from the American Type Culture Collection (ATCC, Manassas, VA, USA). Cells were cultured in medium (RPMI 1640 for BxPC-3 cells; DMEM medium for HEK293T, A549 cells; EMEM for CCD 841 CoN) supplemented with 10% heat-inactivated FBS, 100 units/mL penicillin, 100 µg/mL streptomycin, and 0.25 µg/mL amphotericin B. Cells were incubated at 37°C with 5% CO_2 in a humidified atmosphere. Mycoplasma testing was performed monthly using the MycoAlert mycoplasma detection kit (Lonza, Basel, Switzerland) and all lines were negative.

$p53^{Y220C}$ Reporter Assay

p53 luciferase reporter lentivirus (BPS Bioscience, San Diego, CA, USA) was used to transduce BxPC-3 cells cultured as described above, and tranductants were selected by growth in 1 µg/mL puromycin (Gibco Invitrogen Corp., Grand Island, NY, USA) added directly to the culture medium. Briefly, cells were seeded in 384-well plates (Corning, Corning, NY, USA, cat. no. 3570) and incubated overnight. Subsequently, the cells were treated with the indicated concentrations of compounds. After 24 h, the plates were subjected to Bright-Glo Luciferase Assay System (Promega, Madison, WI, USA) as described in the manufacturer's manual. The proliferation assays were performed in technical triplicate, and data from biological replicates are plotted in GraphPad PRISM 10.3.0.

Cell Viability Assay (CellTiter-Glo Assay)

Cell viability was evaluated using the CellTiter-Glo assay (Promega). Briefly, cells were seeded in 384-well plates and incubated overnight. Subsequently, the cells were treated with the indicated concentrations of compounds. After 72 or 120 h, the plates were subjected to CellTiter-Glo as described in the manufacturer's manual. The proliferation assays were performed in technical

triplicate. IC_{50} values were determined with biological replicates using a non-linear regression curve fit in GraphPad PRISM 10.3.0.

Western Blotting Analysis

Total cell lysates were prepared in 2× sample loading buffer (i.e., 250 mM Tris-hydrochloride: pH 6.8, 4% sodium dodecyl sulfate, 10% glycerol, 0.006% bromophenol blue, 2% β-mercaptoethanol, 50 mM sodium fluoride, and 5 mM sodium orthovanadate). The samples with cell lysates were boiled for 5-8 min at 95°C. The protein concentrations of the cell lysates were quantified using the BCA method and a BCA Protein Assay Kit (Thermo Fisher Scientific, Waltham, MA, USA). Equal amounts of protein were subjected to 4-20% sodium dodecyl sulfate-polyacrylamide gel electrophoresis and transferred to polyvinylidene fluoride membranes (Millipore, Bedford, MA, USA) activated with 100% methanol. The membranes were blocked using Intercept (TBS) Blocking Buffer (LI-COR Biosciences, Lincoln, NE, USA), and subsequently probed with appropriate primary antibodies at 4°C overnight and then incubated with IRDye 800-labeled goat anti-rabbit IgG (LI-COR Biosciences, cat. no. 926-32211) or IRDye 680RD goat anti-Mouse IgG (LI-COR Biosciences, cat. no. 926-68070) secondary antibodies at room temperature for 1 h. After washing the membranes with PBS for 30 min, the membranes were detected on the Li-COR Odyssey CLx system.

Primary antibodies used in this study: anti-FLAG M2 (1:1000, cat. no. F1804; Sigma-Aldrich, Monoclonal), anti-V5-Tag (1:1000, cat. no. 13202; Cell Signaling Technology, Monoclonal), anti-BRD4 (1:1000, cat. no. 63759; Cell Signaling Technology, Monoclonal), anti-p53 (1:1000, cat. no. 18032; Cell Signaling Technology, Monoclonal), anti-Puma (1:1000, cat. no. 12450; Cell Signaling Technology, Monoclonal), anti-Bax (1:1000, cat. no. 5023; Cell Signaling Technology, Monoclonal), anti-p21 (1:1000, cat. no. 2946; Cell Signaling Technology, Monoclonal), anti-MDM2 (1:1000, cat. no. 86934; Cell Signaling Technology, Monoclonal), anti-α-Tubulin (1:5000, cat. no. 3873; Cell Signaling Technology, Monoclonal), anti-GAPDH (1: 5000, cat. no. 2118; Cell Signaling Technology, Monoclonal), and anti-β-Actin (1:5000, cat. no. 4970; Cell Signaling Technology, Monoclonal).

Co-Immunoprecipitation

HEK293T cells were seeded into a 6-well plate (8×10^5 cells/well), cultured overnight, and transfected with 1.5 μg FLAG-tagged full-length BRD4 and 1.5 μg V5-tagged $p53^{Y220C}$ plasmids using TransIT-LT1 transfection reagents (Mirus Bio, Madison, WI, USA). The transfected cells were cultured for another 48 h and treated with either compound or DMSO for 4 h before collection. The cells were collected and lysed in Pierce IP Lysis Buffer (Thermo Fisher Scientific) with cOmplete Mini Protease Inhibitor Cocktail (Roche, Basel, Switzerland) for 30 min on ice and centrifuged for 30 min at 4°C to remove the insoluble fraction. For immunoprecipitation, 20 μL of pre-cleaned anti-FLAG M2 magnetic beads (Sigma-Aldrich, St. Louis, MO, USA) were added to the lysates. The beads–lysate mix was incubated at 4°C overnight on a rotator. Beads were magnetically removed and washed three times with PBS, and the FLAG-Tagged protein was competitively eluted using 3X FLAG Peptide (ApexBio Technology, Houston, TX, USA). Immunoblotting was carried out as described in the Western Blotting Analysis section.

Reverse Transcription Quantitative PCR (RT-qPCR)

Total RNA was extracted using the Direct-zol RNA MicroPrep kit (Zymo Research, Irvine, CA, USA, cat. no. R2062). 1 μg of total RNA was used for synthesizing complementary DNAs (cDNAs) using RevertAid Reverse transcriptase (Thermo Fisher Scientific, cat. no. K1622). The synthesized cDNAs were then diluted 5 times in nuclease-free water and stored at –80°C until used. The diluted cDNAs were used for quantitative PCR in triplicate using PowerUP SYBR green master mix (Thermo Fisher Scientific, cat. no. A25743) and a 7900HT Fast Real-Time PCR machine (Applied Biosystems, Waltham, MA, USA). Expression analysis was performed using specific primers (designed using NCBI's Primer Blast tool or based on reported literatures[53-57]) to amplify each target gene (Supplementary Data 1). The housekeeping gene *GAPDH* used as an internal control to normalize the variability in each sample. All RT-qPCR reactions were conducted at 50°C for 2 min, 95°C for 2 min, and then 40 cycles of 95°C for 15 sec and 60°C for 1 min. The expression level of target genes was quantified using a standard curve. The assay was performed in technical triplicate.

Expression and Purification of Human $p53^{WT}$ and $p53^{Y220C}$

Human $p53^{WT}$ and $p53^{Y220C}$ (residues 94–312) were expressed as 6X His-Spy-TEV fusion proteins in *Escherichia coli* Rosetta DE3 cells. Cells were cultured in Terrific Broth (TB) media

supplemented with kanamycin (100 μg/mL) at 37°C with shaking at 130 rpm. Bacterial cultures were grown to an OD_{600} of 1.2 and induced with 1 mM isopropyl β-D-1-thiogalactopyranoside (IPTG) supplemented with 200 μM $ZnSO_4$ at 18°C overnight. Cells were harvested by centrifugation at 4000 × g for 20 min at 4°C, and the cell pellet was resuspended 5 times w/v in lysis buffer containing 50 mM TRIS pH 8, 200 mM NaCl, 10% glycerol, 1 mM PMSF, and 2.5 mM DTT. After resuspension, cells were lysed by sonication (40% amplitude, 5 sec pulse, 5 sec pause, 5 min total, two times). The lysate was clarified by centrifugation at 75.000 × g for 40 min at 10°C and was then loaded onto a nickel-nitrilotriacetic acid (Ni-NTA) agarose column. Following incubation, the beads were washed with wash buffer containing 50 mM TRIS pH 8, 200 mM NaCl, 20 mM imidazole, and proteins were eluted from the resin in elution buffer containing 50 mM TRIS pH 8, 200 mM NaCl, 500 mM imidazole. The protein was then diluted in 50 mM HEPES pH 7 to lower salt concentration below 50 mM NaCl before being subjected to cation exchange chromatography and eluted in increased salt concentration buffer (50 mM HEPES, 50-1000 mM NaCl, 1 mM TCEP, pH 7). Eluted protein fractions were pooled and concentrated using an Amicon Ultra centrifugal filter (Molecular weight cut-off (MWCO) 10 kDa, Millipore). The concentrated protein was further purified by size-exclusion chromatography using a Superdex 75 16/600 GL column (Cytiva, Marlborough, MA, USA) in buffer containing 50 mM HEPES pH 7, 200 mM NaCl, and 1 mM TCEP. Protein-containing fractions were pooled, and the purity of the protein was assessed by SDS-PAGE. Protein concentration was determined using a Nanodrop. The purified protein was aliquoted, flash-frozen in liquid nitrogen, and stored at -80°C until further use.

Expression and Purification of SpyCatcher S50C

The SpyCatcher S50C expression and purification were performed as previously described[58]. Briefly, SpyCatcher S50C was expressed in *Escherichia coli* Rosetta DE3. Cells were cultured in Luria-Bertani (LB) media supplemented with kanamycin and chloramphenicol (100 μg/mL) at 37°C with shaking at 130 rpm. Bacterial cultures were grown to an OD_{600} of 0.87 and induced with 1 mM IPTG at 18°C overnight. Cells were harvested by centrifugation at 4000 × g for 20 min at 4°C and lysed in the presence of 50 mM Tris-HCl pH 8.0, 200 mM NaCl, 1 mM TCEP, and 1 mM PMSF. Following ultracentrifugation, the soluble fraction was passed over the Ni-NTA agarose column and eluted with elution buffer containing 50 mM Tris-HCl pH 8.0, 200 mM NaCl, 400 mM imidazole, 1 mM TCEP. The affinity-purified protein was subjected to size exclusion

chromatography (SEC), using a Superdex 75 16/600 GL column (Cytiva) equilibrated with SEC buffer (50 mM HEPES pH 7.5, 200 mM NaCl, 0.1 mM TCEP). Eluted protein was concentrated and flash-frozen in liquid nitrogen.

Labeling of SpyCatcher S50C with BODIPY-FL-maleimide

Labeling of SpyCatcher with BODIPY-FL-maleimide was performed as previously described[58]. Briefly, purified SpyCatcher S50C protein was incubated with DTT (8 mM) at 4°C for 1 h. DTT was removed using a Superdex 75 16/600 GL size exclusion column in a buffer containing 50 mM TRIS pH 7.5, 150 mM NaCl, and 0.1 mM TCEP. BODIPY-FL-maleimide (Thermo Fisher) was dissolved in 100% DMSO and mixed with SpyCatcher S50C to achieve a 1.1 molar excess of BODIPY-FL-maleimide. SpyCatcher S50C labeling was carried out overnight at 4°C. The labeled SpyCatcher S50C was then purified on a Superdex 75 16/600 GL size exclusion column (Cytiva) in buffer containing 50 mM Tris pH 7.5, 150 mM NaCl, and 1 mM TCEP. The purified protein was concentrated using an Amicon Ultra centrifugal filter (Millipore), flash-frozen in liquid nitrogen, and stored at -80°C.

Labeling of $p53^{WT}$ and $p53^{Y220C}$ with BODIPY-FL-SpyCatcher S50C

Purified $p53^{WT}$ or $p53^{Y220C}$ mutant proteins were incubated overnight at 4°C with BODIPY-FL labeled SpyCatcher S50C protein at a stoichiometric ratio. Protein was concentrated and loaded on the Superdex 75 10/300 size exclusion column (Cytiva). Labeling was monitored with absorption at 280 and 490 nm. The protein peak corresponding to the labeled protein was pooled, concentrated using an Amicon Ultra centrifugal filter (Millipore), flash-frozen (7.9 μM for p53-WT-SpyCatcher-S50C-BODIPY-FL and 2.4 μM for p53-Y220C-SpyCatcher-S50C-BODIPY-FL) in liquid nitrogen, and stored at -80°C.

Expression, Purification and Biotinylation of $BRD4_{BD1}$

$BRD4_{BD1}$ was expressed in *Escherichia coli* Rosetta DE3. Cells were cultured in Luria-Bertani (LB) media supplemented with kanamycin and chloramphenicol (100 μg/mL) at 37°C with shaking at 130 rpm. Bacterial cultures were grown to an OD_{600} of 0.6 and induced with 1 mM IPTG at 18°C overnight. Cells were harvested by centrifugation at 4000 × g for 20 min at 4°C and lysed in the presence of 50 mM Tris-HCl pH 8.0, 200 mM NaCl, 10 mM imidazole, 1 mM TCEP,

1 mM PMSF, and 0.1% TritonX-100. Following ultracentrifugation, the soluble fraction was passed over the Ni-NTA agarose column and eluted with elution buffer containing 50 mM Tris-HCl pH 8.0, 200 mM NaCl, and 100 mM imidazole. The $BRD4_{BD1}$ protein was biotinylated in vitro in the presence of 500 nM BirA enzyme, 10 mM $MgCl_2$, 200 µM biotin, and 20 mM ATP in an SEC buffer containing 50 mM HEPES pH 7.5, 200 mM NaCl, and 1 mM TCEP for 1 h at room temperature, following incubation overnight at 4°C. The biotinylated protein was subjected to size exclusion chromatography, using a Superdex 75 16/600 GL column (Cytiva) equilibrated with the SEC buffer. Eluted protein was concentrated and flash-frozen in liquid nitrogen.

Time-Resolved Fluorescence Resonance Energy Transfer (TR-FRET)

Compounds in dimerization assays were dispensed in a 384-well microplate (Corning, cat. no. 4514) using D300e Digital Dispenser (Tecan, Männedorf, Switzerland) normalized to 1% DMSO into 100 nM biotinylated $BRD4_{BD1}$, 100 nM p53-Y220C-BODIPY-FL-SpyCatcher S50C (or 100 nM p53-WT-BODIPY-FL-SpyCatcher S50C) and 2 nM terbium-coupled streptavidin (Invitrogen) in a buffer containing 50 mM Tris pH 7.5, 200 mM NaCl, and 1 mM TCEP. Before the TR-FRET measurements were conducted, the reactions were incubated for 15 min at RT. The plate was then read on a Pherastar FSX (BMG Labtech, Ortenberg, Germany) microplate reader. Following the excitation of terbium fluorescence at 337 nm, emission at 490 nm (terbium) and 520 nm (BODIPY-FL) were recorded and the TR-FRET signal of each data point was calculated as the 520/490 nm ratio. Data from two independent measurements (n=2), each calculated as an average of ten technical replicates per well per experiment, were plotted in GraphPad Prism 10.2.2.

TR-FRET binding assay

To assess binding via a TR-FRET assay, a reaction mixture containing 50 nM p53 Y220C, 600 nM **XJZ-06-618** FITC-labeled tracer, and 1X MAb Anti-6His-Tb antibody (61HI2TLB, Revvity) was prepared in assay buffer (50 mM HEPES pH 7.5, 200 mM NaCl, 0.1% Pluronic F-68, 0.5 mg/ml BSA). This mixture was dispensed into a 384-well microplate (Corning, cat. no. 4514). Test compounds were then directly added to the same plate using a D300e Digital Dispenser (Tecan), and normalized to a final DMSO concentration of 1%. Following compound addition, the plate was incubated at room temperature (RT) for 15 minutes to allow binding equilibrium. TR-FRET measurements were then performed using a PHERAstar FSX microplate reader (BMG Labtech).

The TR-FRET signal was calculated as the emission ratio of 520 nm to 490 nm (520/490). Data represent the mean of two independent experiments (n = 2), each with ten technical replicates per condition. Cooperativity was calculated by determining the ratio of IC_{50} values for the condition in the absence and presence of BRD4 protein. Results were analyzed and visualized using GraphPad Prism version 10.2.2.

Nano Differential Scanning Fluorimetry (NanoDSF)

Thermal unfolding experiments were carried out by nanoDSF (Prometheus NT.48). For all measurements, 15 µL samples were prepared containing 15 µM protein and 50 µM of tested compound. The remaining volume was filled up with buffer containing 50 mM HEPES, 200 mM NaCl, 1 mM TCEP, pH 7). The prepared sample was filled into the capillaries by capillary force action and then placed into the instrument. The capillaries were heated from 15 to 70 °C with a heating rate of 2 °C /min, and the changes in the fluorescence ratio (F350/F330) as a function of temperature were monitored to determine the apparent thermal stability (T_m).

Construction of pX459 TP53 Vector

pX459-TP53 vector was generated by cloning sgRNA targeting human *TP53* into the pX459 (Addgene #62988). *TP53*-targeted guide RNA was designed using the designing tool at https://chopchop.cbu.uib.no/. The backbone pX459 plasmid was cut with BbsI digestion enzyme and ligated to complementary annealed oligos containing the BbsI overhang site and *TP53* sgRNA sequence. The oligo sequences which target *TP53* were: 5'-CACCGCGACGCTAGGATCTGACTG-3' and AAACCAGTCAGATCCTAGCGTCGC-3'.

Generation of A549 TP53 Knockout (A549-p53$^{-/-}$) Cell Line

A549 cells were transfected with pX459-*TP53* using lipofectamine 2000 (Invitrogen, cat. no. 11668027) according to manufacturer's instructions. After 48 h of transfection, the transfected cells were passaged and cultured in medium containing 2 µg/mL puromycin (Gibco, cat. no. A11138-03) for three days. The surviving cells were grown for an additional 10 days to form cell colonies. Individual cell colonies were picked and expanded into different clones. Knockout efficiency of p53 in each clone was confirmed using immunoblotting with anti-p53 antibody.

Construction of pLenti6/V5-p53_p53^{Y220C}

The pLenti6/V5-p53_p53^{WT} (Addgene #22945) as a backbone plasmid was used as a template for site-directed mutagenesis to generate pLenti6/V5-p53_p53Y220C. KOD Xtreme Hot Start DNA Polymerase (Sigma-Aldrich, cat. no. 71975-M) was used to amplify the template with a pair of primers (Forward primer 5'-AGTGTGGTGGGTCCTGTGAGCCGCCTGAGGTT-3'; and Reverse primer: 5'-AACCTCAGGCGGCTCACAGGGCACCACACACT-3'), and the mutation was verified by Sanger sequencing.

Generation of A549-p53^{WT} and -p53^{Y220C} Cell Lines

HEK293T cells were transfected with either pLenti6/V5-p53_p53^{WT} (Addgene #22945) or pLenti6/V5-p53_p53^{Y220C}, along with pMD2.G (Addgene #12259)/psPAX2 (Addgene #12260), using TransIT-LT1 transfection reagents (Mirus Bio) to produce lentivirus. After 48 h of transfection, the supernatant was collected, filtered, and added to A549-p53$^{-/-}$ cells in the presence of 5 μg/mL polybrene (APExBIO, cat. No. K2701). Following 48 h of infection, the infected cells were passaged and cultured in medium containing 10 μg/mL blasticidin (Gibco, cat. no. A11139-03) for five days. The surviving cells were grown for an additional 7 days to form cell colonies. Individual cell colonies were picked and expanded into different clones. The expression p53 in each clone was confirmed using immunoblotting with anti-V5 antibody.

BrdU Proliferation Analysis

Cells were cultured on coverslips in RPMI (10 % FBS, 1 % penicillin and streptomycin) media. Cells were then treated with the indicated compounds for 24 h prior to pulse with BrdU (ab142567, Abcam, 10 μg/mL) for 4 h. After that, cells were fixed with 4% paraformaldehyde for 15 min and permeabilized with 0.5 % Triton X-100 for 10 min. DNA was then denatured by treating the fixed cells with 1.5N HCl for 10 min. Cells were blocked in 5% BSA for 1 h at room temperature and stained with primary antibody toward BrdU (ab152095; Abcam, 1:200 dilution) overnight at 4^{o}C. On the next day, cells were incubated with the secondary antibody Alexa Fluor 680 goat anti-rabbit IgG (A-21076; Invitrogen, 1:1000). Cells were visualized using a Nikon Ti2-E fluorescent microscope. BrdU^{+} cells were quantified using ImageJ.

NanoBRET assay for BRD4 engagement

HEK293T cells (8 x 10^5 cells per well) were plated in a 6-well plate overnight. Each well was transfected the next day with 1 μg NanoLuc-BRD4 in 200 μL Opti-MEM™ (Gibco) using FuGENE HD (Promega) according to manufacturer's recommendations. The cells were incubated overnight and divided into two pools with the addition of NanoBRET Intracellular TE BET BRD Tracer (Promega) at 100 nM in one pool the following day. Then, cells were replated in an opaque white 384-well plate (Corning) at 2 x 10^5 cells/mL (40 μL/well) in Opti-MEM™ I Reduced Serum Medium, no phenol red (Gibco) with 4% FBS and incubated overnight. The next day, cells were treated with the indicated compounds in triplicate for 2 h. A mixture containing 30 uL Nano-Glo Substrate and 10 uL Extracellular NanoLuc Inhibitor in 4960 uL Opti-MEM™ I Reduced Serum Medium, no phenol red was prepared freshly and was added to each well (20 μL/well). The plate was immediately read on a PHERAStar plate reader (BMG LABTECH) using a LUM 610-LP 450-80 optical module. The BRET ratio was calculated according to the manufacturer's instructions, and graphs were obtained using the GraphPad Prism non-linear regression curve fit function by considering each set of measurements as an independent replicate for curve fitting.

Sample Preparation for RNA Sequencing (RNA-Seq)

BxPC-3 cells were seeded into a 6-well plate (5×10^5 cells/well), cultured overnight, treated with indicated compounds for either 2 or 4 h, and harvested with TRIzol (Invitrogen). Total RNA was extracted using the Direct-zol RNA MicroPrep kit (Zymo Research) according to manufacturer's instructions. For sequencing library preparation, polyA-containing transcripts were enriched, prepared into paired-end libraries, and sequenced on an Illumina NovaSeq using paired-end 150-bp read length by Novogene. (Durham, NC, USA).

RNA-seq Analysis

RNA sequencing data was processed using the nf-core/rnaseq pipeline (v3.18.0). Adaptor trimming was performed using Trim Galore! (0.6.10), reads were aligned using STAR (2.6.1d) and quantified using Salmon (1.10.3). Quality control checks were performed using FASTQC (0.12.1) and RSeQC (5.0.2). Differential expression analysis and gene set enrichment analysis were performed in R using DESeq2 (1.38.3) and fgsea (1.24.0), respectively. For each DESeq comparison, log fold change shrinkage was applied using the "ashr" method, and genes were

ranked by shrunk log fold change values. The HALLMARK_P53_PATHWAY gene set was obtained from MSigDB (5.0). The list of p53 target genes was obtained from Fischer 2017 Table 1[43]. All plots for the RNA sequencing analysis were created in R using ggplot2 (3.5.1).

Senescence Stain

SA-β-Galactosidase Staining was performed with a kit (Cell signaling Technology, Cat. 9860), according to the manufacturer's protocol.

Apoptosis Fluorescence Activated Cell Sorting (FACS)

Cells were harvested by trypsinization and washed once with 1x PBS and once with 1x binding buffer (0.1M Hepes, 1.4M NaCl, and 25 mM $CaCl_2$). Cells for each sample were resuspended in 100 ul 1x binding buffer with 5 ul FITC-annexin V (BioLegend, Cat. No. 640945) and incubated for 10-15 mins at room temperature (protected from light). Cells were then washed and resuspended into 100 ul of 1x binding buffer after incubation. 5 ul of propidium iodide was added to each sample and incubated for 5 mins at room temperature. Then samples were analyzed with flow cytometry.

DATA AVAILABILITY

RNA-seq data are available from the NCBI Gene Expression Omnibus with the dataset identifier GSE322557 [https://www.ncbi.nlm.nih.gov/geo/query/acc.cgi?acc=GSE322557] (Effect of TRAP-1 and control compounds on gene expression in BxPC-3 cells). The data generated in this study are provided in the Supplementary Information/Source Data file. Source data are provided with this paper.

REFERENCES

1. Lavin, M.F. & Gueven, N. The complexity of p53 stabilization and activation. *Cell Death Differ* **13**, 941-50 (2006).
2. Boutelle, A.M. & Attardi, L.D. p53 and Tumor Suppression: It Takes a Network. *Trends Cell Biol* **31**, 298-310 (2021).
3. Kastenhuber, E.R. & Lowe, S.W. Putting p53 in Context. *Cell* **170**, 1062-1078 (2017).
4. Martincorena, I. & Campbell, P.J. Somatic mutation in cancer and normal cells. *Science* **349**, 1483-9 (2015).
5. Olivier, M. et al. The IARC TP53 database: new online mutation analysis and recommendations to users. *Hum Mutat* **19**, 607-14 (2002).

6. Wang, M. & Attardi, L.D. A Balancing Act: p53 Activity from Tumor Suppression to Pathology and Therapeutic Implications. *Annu Rev Pathol* **17**, 205-226 (2022).
7. Wang, H., Guo, M., Wei, H. & Chen, Y. Targeting p53 pathways: mechanisms, structures, and advances in therapy. *Signal Transduct Target Ther* **8**, 92 (2023).
8. Vassilev, L.T. et al. In vivo activation of the p53 pathway by small-molecule antagonists of MDM2. *Science* **303**, 844-8 (2004).
9. Iancu-Rubin, C. et al. Activation of p53 by the MDM2 inhibitor RG7112 impairs thrombopoiesis. *Exp Hematol* **42**, 137-45.e5 (2014).
10. Mahfoudhi, E. et al. P53 activation inhibits all types of hematopoietic progenitors and all stages of megakaryopoiesis. *Oncotarget* **7**, 31980-92 (2016).
11. Hassin, O. & Oren, M. Drugging p53 in cancer: one protein, many targets. *Nat Rev Drug Discov* **22**, 127-144 (2023).
12. Joerger, A.C., Ang, H.C. & Fersht, A.R. Structural basis for understanding oncogenic p53 mutations and designing rescue drugs. *Proc Natl Acad Sci U S A* **103**, 15056-61 (2006).
13. Petitjean, A. et al. Impact of mutant p53 functional properties on TP53 mutation patterns and tumor phenotype: lessons from recent developments in the IARC TP53 database. *Hum Mutat* **28**, 622-9 (2007).
14. Bray, F. et al. Global cancer statistics 2022: GLOBOCAN estimates of incidence and mortality worldwide for 36 cancers in 185 countries. *CA Cancer J Clin* **74**, 229-263 (2024).
15. Boeckler, F.M. et al. Targeted rescue of a destabilized mutant of p53 by an in silico screened drug. *Proc Natl Acad Sci U S A* **105**, 10360-5 (2008).
16. Wilcken, R. et al. Halogen-enriched fragment libraries as leads for drug rescue of mutant p53. *J Am Chem Soc* **134**, 6810-8 (2012).
17. Bauer, M.R. et al. A structure-guided molecular chaperone approach for restoring the transcriptional activity of the p53 cancer mutant Y220C. *Future Med Chem* **11**, 2491-2504 (2019).
18. Levine, A., Mack, D., Vu, B., Davis, T.W. & Dumble, M. Methods and Compounds for Restoring Mutant p53 Function. (PMV Pharmaceuticals, Inc., United States, 2021).
19. Li, S. et al. Heteroarylalkyne compounds for targeting mutant of p53 and their preparation. (Jacobio Pharmaceuticals Co., Ltd., China, 2023).
20. Vu, B.T. et al. Discovery of Rezatapopt (PC14586), a First-in-Class, Small-Molecule Reactivator of p53 Y220C Mutant in Development. *ACS Med Chem Lett* **16**, 34-39 (2025).
21. Puzio-Kuter, A.M. et al. Restoration of the Tumor Suppressor Function of Y220C-Mutant p53 by Rezatapopt, a Small Molecule Reactivator. *Cancer Discov* (2025).
22. Guiley, K.Z. & Shokat, K.M. A Small Molecule Reacts with the p53 Somatic Mutant Y220C to Rescue Wild-type Thermal Stability. *Cancer Discov* **13**, 56-69 (2023).
23. Stanton, B.Z., Chory, E.J. & Crabtree, G.R. Chemically induced proximity in biology and medicine. *Science* **359**(2018).
24. Singh, S. et al. Proximity-inducing modalities: the past, present, and future. *Chem Soc Rev* **52**, 5485-5515 (2023).
25. Kong, L. et al. Selective degradation of the p53-R175H oncogenic hotspot mutant by an RNA aptamer-based PROTAC. *Clin Transl Med* **13**, e1191 (2023).
26. Wang, W.W. et al. Targeted Protein Acetylation in Cells Using Heterobifunctional Molecules. *J Am Chem Soc* **143**, 16700-16708 (2021).

27. Kabir, M. et al. Acetylation Targeting Chimera Enables Acetylation of the Tumor Suppressor p53. *J Am Chem Soc* **145**, 14932-14944 (2023).
28. Kabir, M. et al. Harnessing the TAF1 Acetyltransferase for Targeted Acetylation of the Tumor Suppressor p53. *Adv Sci (Weinh)* **12**, e2413377 (2025).
29. Liu, J. et al. TF-DUBTACs Stabilize Tumor Suppressor Transcription Factors. *J Am Chem Soc* **144**, 12934-12941 (2022).
30. He, C. et al. Construction of Small-Molecule Deubiquitinase-Targeting Chimeras to Reactivate and Stabilize Mutant p53 Y220C in Vitro and in Vivo. *Angew Chem Int Ed Engl* **65**, e18249 (2026).
31. Sadagopan, A. et al. Mutant p53 protein accumulation is selectively targetable by proximity-inducing drugs. *Nat Chem Biol* (2025).
32. Gourisankar, S. et al. Rewiring cancer drivers to activate apoptosis. *Nature* **620**, 417-425 (2023).
33. Sarott, R.C. et al. Relocalizing transcriptional kinases to activate apoptosis. *Science* **386**, eadl5361 (2024).
34. Izetti, P. et al. PRIMA-1, a mutant p53 reactivator, induces apoptosis and enhances chemotherapeutic cytotoxicity in pancreatic cancer cell lines. *Invest New Drugs* **32**, 783-94 (2014).
35. Vu, B., Dominique, R. & Li, H. Methods and Compounds for Restoring mutant p53 function. (PMV Pharmaceuticals, Inc., 2017).
36. Filippakopoulos, P. et al. Selective inhibition of BET bromodomains. *Nature* **468**, 1067-73 (2010).
37. Erwin, G.S. et al. Synthetic transcription elongation factors license transcription across repressive chromatin. *Science* **358**, 1617-1622 (2017).
38. Chiarella, A.M. et al. Dose-dependent activation of gene expression is achieved using CRISPR and small molecules that recruit endogenous chromatin machinery. *Nat Biotechnol* **38**, 50-55 (2020).
39. Gibson, W.J. et al. Bifunctional Small Molecules That Induce Nuclear Localization and Targeted Transcriptional Regulation. *J Am Chem Soc* **145**, 26028-26037 (2023).
40. Mack, E.T., Perez-Castillejos, R., Suo, Z. & Whitesides, G.M. Exact analysis of ligand-induced dimerization of monomeric receptors. *Anal Chem* **80**, 5550-5 (2008).
41. Vu, B. & Good, A. Uses of p53 X-ray co-crystal structures. (PMV Pharmaceuticals, Inc., United States, 2023).
42. Sarott, R. et al. Borrowing Transcriptional Kinases to Activate Apoptosis. *bioRxiv*, 2023.10.23.563687 (2023).
43. Fischer, M. Census and evaluation of p53 target genes. *Oncogene* **36**, 3943-3956 (2017).
44. Bradner, J.E., Hnisz, D. & Young, R.A. Transcriptional Addiction in Cancer. *Cell* **168**, 629-643 (2017).
45. Darnell, J.E. Transcription factors as targets for cancer therapy. *Nat Rev Cancer* **2**, 740-9 (2002).
46. Bushweller, J.H. Targeting transcription factors in cancer - from undruggable to reality. *Nat Rev Cancer* **19**, 611-624 (2019).
47. Bieging, K.T., Mello, S.S. & Attardi, L.D. Unravelling mechanisms of p53-mediated tumour suppression. *Nat Rev Cancer* **14**, 359-70 (2014).
48. Wang, M. et al. p53 drives lung cancer regression through a TSC2/TFEB-dependent senescence program. *Cancer Discov* (2025).

49. Latif, A.L. et al. BRD4-mediated repression of p53 is a target for combination therapy in AML. *Nat Commun* **12**, 241 (2021).
50. Altinbay, M. et al. Chem-CRISPR/dCas9FCPF: a platform for chemically induced epigenome editing. *Nucleic Acids Res* **52**, 11587-11601 (2024).
51. Kelley, C. et al. p53Y220C-BET-bifunctionals (tPRIMEs) drive p53Y220C-mutant cancer cells into apoptosis. *bioRxiv*, 2025.08.13.669398 (2025).
52. Alerasool, N., Leng, H., Lin, Z.Y., Gingras, A.C. & Taipale, M. Identification and functional characterization of transcriptional activators in human cells. *Mol Cell* **82**, 677-695.e7 (2022).
53. Van Nostrand, J.L. et al. Inappropriate p53 activation during development induces features of CHARGE syndrome. *Nature* **514**, 228-32 (2014).
54. Singh, S. et al. Human oncoprotein MDM2 activates the Akt signaling pathway through an interaction with the repressor element-1 silencing transcription factor conferring a survival advantage to cancer cells. *Cell Death Differ* **20**, 558-66 (2013).
55. Lynch, J.T. et al. The role of glucocorticoid receptor phosphorylation in Mcl-1 and NOXA gene expression. *Mol Cancer* **9**, 38 (2010).
56. Salari Fanoodi, T., Motalleb, G., Yegane Moghadam, A. & Talaee, R. p21 Gene Expression Evaluation in Esophageal Cancer Patients. *Gastrointestinal Tumors* **2**, 144-164 (2015).
57. Garrison, S.P. et al. Selection against PUMA gene expression in Myc-driven B-cell lymphomagenesis. *Mol Cell Biol* **28**, 5391-402 (2008).
58. Nowak, R.P. et al. Plasticity in binding confers selectivity in ligand-induced protein degradation. *Nat Chem Biol* **14**, 706-714 (2018).

ACKNOWLEDGEMENTS

This work was supported by the National Institutes of Health (NIH) grant NIH High End Instrumentation grant (1S10OD028697-01) (to N.S.G.), R35 grant CA197591 (to L.D.A.), departmental funds from Stanford Chemical and Systems Biology and Stanford Cancer Institute (to N.S.G.), Ludwig Institute, Stanford's SPARK Translational Research Program, and Bio-X. This work was supported by the National Research Foundation of Korea (NRF) grant funded by the Korea government (MSIT) (RS-2026-25469433) (to W.S.B.). R.P.N. is a member of the excellence cluster ImmunoSensation2 funded by the Deutsche Forschungsgemeinschaft (DFG) under Germany's Excellence Strategy (EXC2151–390873048). R.C.S. acknowledges the Swiss National Science Foundation for a postdoctoral fellowship (SNF Mobility grant P500PN_206898). M.W. acknowledges the Tobacco Related Diseases Research Program for a postdoctoral fellowship award (TRDRP T31FT1610). S.G. was supported by NIH NCI 1K99CA296700-01.

AUTHOR CONTRIBUTIONS

X.Z., W.S.B., and D.E.P. contributed equally to this work. X.Z., W.S.B., and N.S.G. conceived and initiated the study; X.Z. designed and synthesized bivalent compounds with the help of J.Z., Q.G., R.C.S., and T.Z.; W.S.B. designed and conducted cell biological experiments with the help of M.W., K.T.N., S.A.N, S.G., N.A.P., T.Q., and Z.J.; D.E.P. carried out biochemical studies. J.G. assisted with protein purification; N.S.G., R.P.N., and L.D.A. supervised the project; The manuscript was written by X.Z., W.S.B., D.E.P., S.M.H., and N.S.G. with input from all authors.

COMPETING INTERESTS

N.S.G. is a founder, science advisory board member (SAB) and equity holder in Syros, C4, Allorion, Lighthorse, Inception, Matchpoint, Shenandoah (board member), Larkspur (board member) and Soltego (board member). The Gray lab receives or has received research funding from Novartis, Takeda, Astellas, Taiho, Jansen, Kinogen, Arbella, Deerfield, Springworks, Interline and Sanofi. T.H.Z is a consultant for K2 Medicine. All other authors declare no competing interests.

Figure 1: Chemical Targeting of p53 in Cancer Cells. A. Schematic of the traditional occupancy-based approach to develop MDM2 inhibitors that interrupt the MDM2-$p53^{WT}$ interaction (left) and $p53^{Y220C}$ correctors that bind to $p53^{Y220C}$ and increase its thermal stability (right). **B.** Schematic of the event-driven transcriptional activator of p53 (TRAP) targeting $p53^{Y220C}$ mutant through the recruitment of BRD4.

Figure 2: Development of B-1-based bivalent TRAPs. A. The structures of the B-1-based TRAP library. **B.** TR-FRET. The ternary complex formation measured by TR-FRET between purified $p53^{Y220C}$ and $BRD4_{BD1}$. The data is shown as means of n=2 biological replicates. **C.** Luciferase reporter. Activation of p53-regulated transcription in BxPC-3 ($p53^{Y220C}$) cells after compound treatment for 24 h. The data is shown as means of n=2 biological replicates. Source data are provided as a Source Data file.

Figure 3: Ternary complex formation is required for TRAP-mediated transcription activation. A. Structures of negative controls containing minor chemical modifications to remove BRD4 binding (**TRAP-1-NegB**) or $p53^{Y220C}$ binding (**TRAP-1-NegP**). **B.** NanoDSF measurements quantifying $p53^{Y220C}$ thermal stability with the indicated compounds included. The data is shown as means of n=2 biological replicates. **C.** TR-FRET. The ternary complex formation of TRAPs and their negative controls measured by TR-FRET between $p53^{Y220C}$ and $BRD4_{BD1}$. The data is shown as means of n=2 biological replicates. **D.** Luciferase reporter. The p53-regulated transcriptional activation of TRAPs and their negative controls at 24 h in BxPC-3 cells. The data is shown as means of n=2 biological replicates. **E.** The co-immunoprecipitation of TRAPs compared with the cotreatment of $p53^{Y220C}$ binder (**B-1 linker**) and BRD4 binder (JQ1) in HEK293T cells after 4 h of compound treatment. Western blot experiments were independently repeated at least twice with similar results. Source data are provided as a Source Data file.

Figure 4: Activation of p53 target gene transcription. A. RT-qPCR. Changes of gene expression after 3 µM **TRAP-1** incubation for 8 h in BxPC-3 cells compared with the controls. A representative set of data is shown with mean ± s.d. of n=3 technical replicates. **B.** Differential expression and gene set enrichment plot of the HALLMARK_P53_PATHWAY gene set in BxPC-3 cells treated with DMSO or 3 µM compounds for 2 h and 4 h in triplicate. Padj = adjusted p value. NES = normalized enrichment score. Gene set enrichment analysis was performed using the fgsea R package with Hallmark gene sets from MSigDB. Genes were ranked by shrunken log fold change from differential expression analysis. Significance was assessed using permutation testing implemented in fgsea, and p-values were adjusted for multiple testing using the Benjamini-Hochberg false discovery rate method. **C.** Heatmap enrichment in high-confidence p53-target genes[43] (Top 1-50 genes). BxPC-3 cells were treated with DMSO or 3 µM compounds for 4 h in triplicate. FC = fold change. **D.** Changes in protein level after treatment with TRAPs at 16 h in BxPC-3 cells compared with the controls. Western blot experiments were independently repeated at least twice with similar results. **E.** p21 protein level changes after TRAPs treatment at 2 h in BxPC-3 cells compared with the controls. Western blot experiments were independently repeated at least twice with similar results. Source data are provided as a Source Data file.

Figure 5: TRAP-1 induces senescence and apoptosis. A. Washout experiment. BxPC-3 cells were incubated with 2 μM TRAPs and controls for 2 h, followed by a washout. Cell proliferation was measured 72 h after washout. A representative set of data is shown with box plots display the medium (centre line), interquartile range (box bounds) and minima/maxima (whiskers) (n = 48 technical replicates). P values were calculated by one-way ANOVA with the Turkey test *post hoc* test for pairwise comparison. **TRAP-1** vs. **B-1 linker**, $P = 2.87 \times 10^{-13}$ (significant); **TRAP-1** vs. DMSO, $P = 2.87 \times 10^{-13}$ (significant); **B-1 linker** vs. DMSO, $P = 3.42 \times 10^{-13}$ (significant). **B.** p21 protein level changes in the washout experiment. The expression was measured 24 h after washout. Western blot experiments were independently repeated at least twice with similar results. **C.** Representative immunofluorescence images of the BrdU staining experiment. BxPC-3 cells were imaged upon 24 h treatment of 3 μM **TRAP-1** compared with controls. Scale bar, 100 μm. **D.** Quantification of BrdU incorporated BxPC-3 cells. The data is shown with means ± s.d. of n=3 biological samples. P values were calculated by one-way ANOVA with the Turkey test *post hoc* test for pairwise comparison. **TRAP-1** vs. DMSO, P = 0.0011 (significant); **TRAP-1** vs. **TRAP-1-NegB**, P = 0.0031 (significant); **TRAP-1** vs. **TRAP-1-NegP**, P = 0.0107 (significant). **E.** Representative images of SA-β-galactosidase (SA-β-gal) staining experiment. A549-p53^{Y220C} cells were imaged upon 6-day treatment of 3 μM **TRAP-1** compared with controls. Scale bar, 100 μm. **F**. Quantification of analysis showing percentage of SA-β-gal positive cells among all cells per 100X field. A representative set of data is shown with means ± s.d. of n=5 technical replicates. P values were calculated by one-way ANOVA with the Turkey test *post hoc* test for pairwise comparison. **TRAP-1** vs. DMSO, $P = 3.63 \times 10^{-13}$ (significant). **G.** Quantification of FACS analyses showing percentage of Annexin V positive cells. A549-p53^{Y220C} cells were imaged upon 5-day treatment of 3 μM **TRAP-1** compared with controls. A representative set of data is shown with means ± s.d. of n=3 technical replicates. P values were calculated by one-way ANOVA with the Turkey test *post hoc* test for pairwise comparison. **TRAP-1** vs. DMSO, $P = 4.72 \times 10^{-12}$ (significant); JQ1 vs. DMSO, $P = 1.78 \times 10^{-10}$ (significant); **TRAP-1** vs. JQ1, P = 0.0012 (significant). Source data are provided as a Source Data file.

Figure 6: The antiproliferative activity of TRAPs in different cell lines. A. The antiproliferative activity of TRAPs compared with weaker or inactive compounds at 72 h in BxPC-3 cells. The data is shown as means of n=2 biological replicates. **B.** Heatmap showing the antiproliferative potency of **TRAP-1** compared with controls in BxPC-3 ($p53^{Y220C}$), A549 ($p53^{WT}$), and CCD 841 CoN ($p53^{WT}$). The data is shown as means ± s.d. of n=2 biological replicates. Source data are provided as a Source Data file.

Editorial Summary
The tumor suppressor protein p53 is commonly mutated in cancer and has been challenging for therapeutic reactivation. Here, the authors developed a small molecule chemical inducer of proximity to selectively activate p53 transcription and induce cellular senescence and apoptosis in $p53^{Y220C}$ cells.

Peer Review Information: *Nature Communications* thanks Peter Kaiser and the other, anonymous, reviewer(s) for their contribution to the peer review of this work. A peer review file is available.

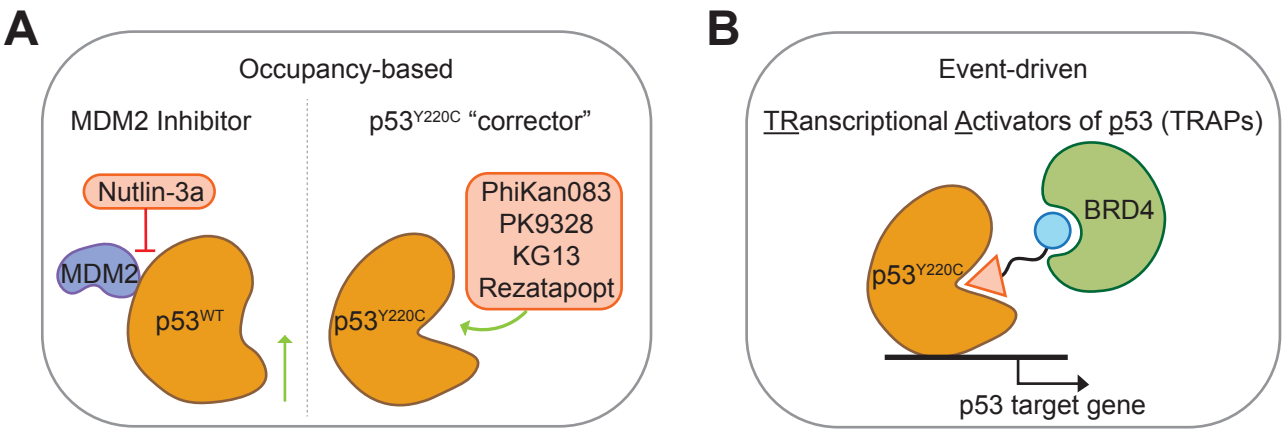

A

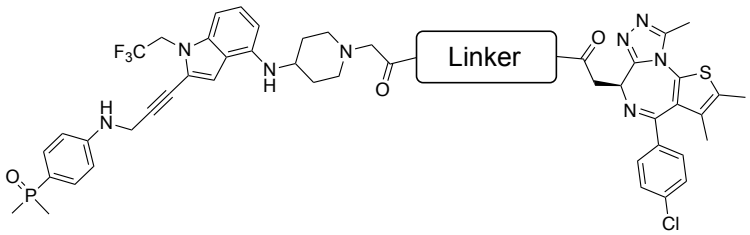

Compound ID (XJZ-06-**XXX**)	Linker
444 (n=4) **445** (n=6) **446** (n=8)	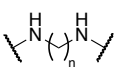
448 (n=2) **449** (n=4)	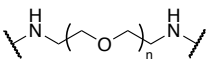
462 **(TRAP-1)**	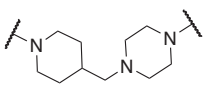
463 **(TRAP-2)**	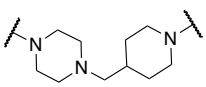
464 **(TRAP-3)**	
465	
471	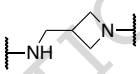
537	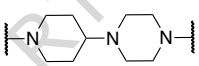
540	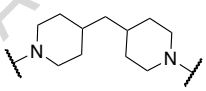

B

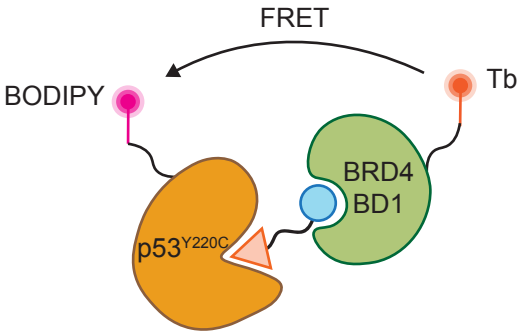

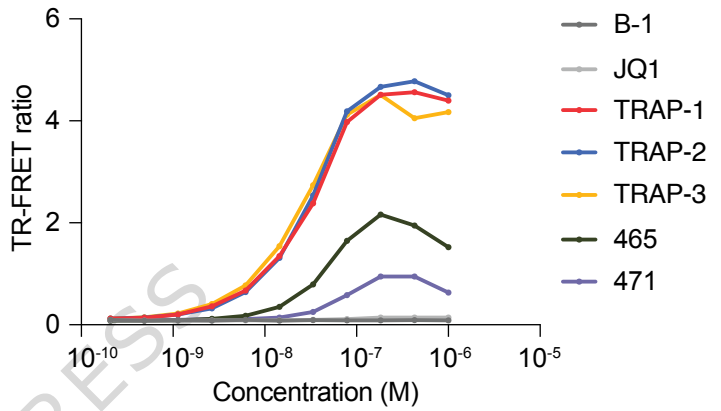

C

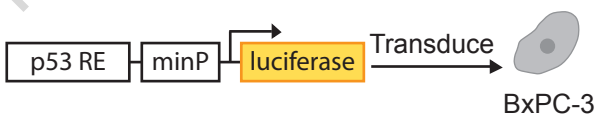

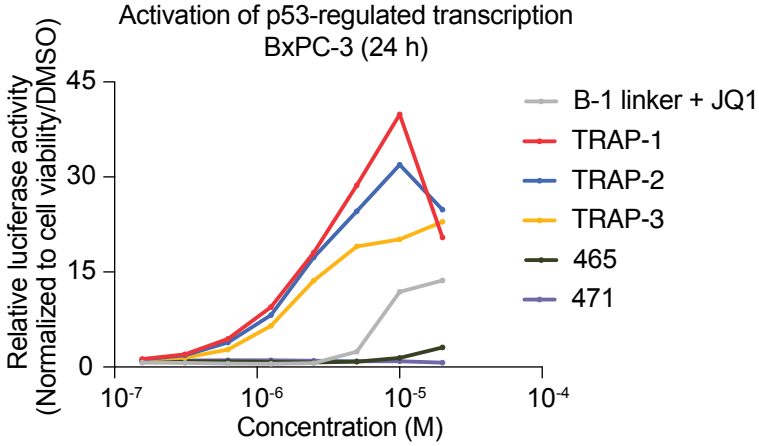

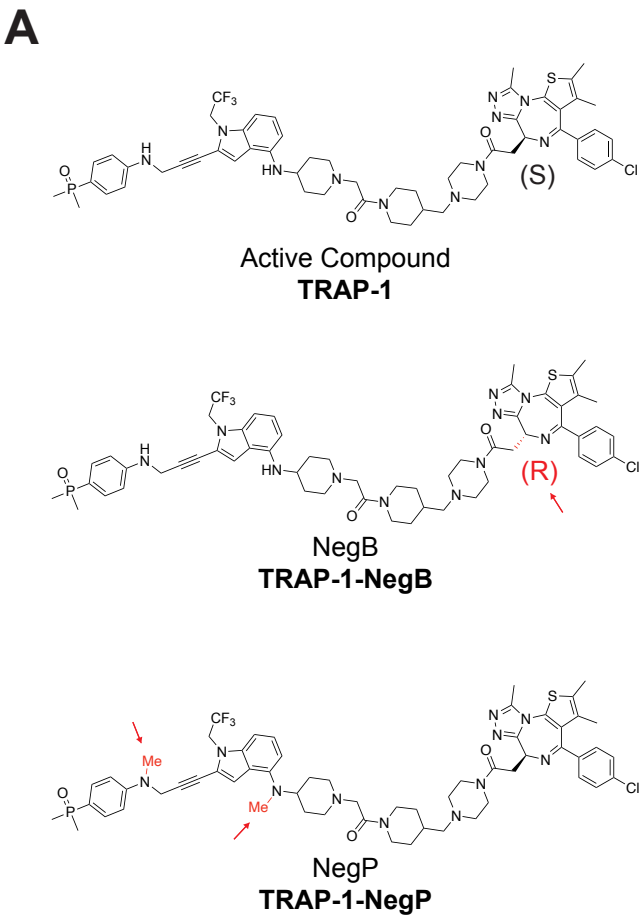

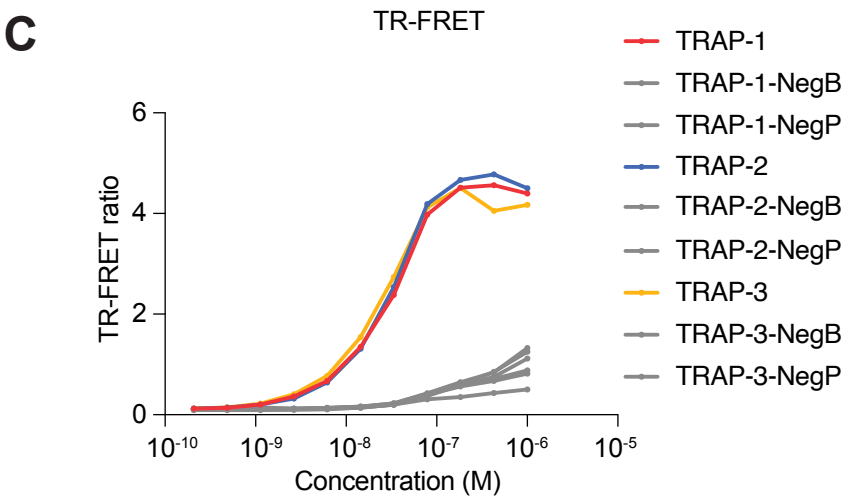

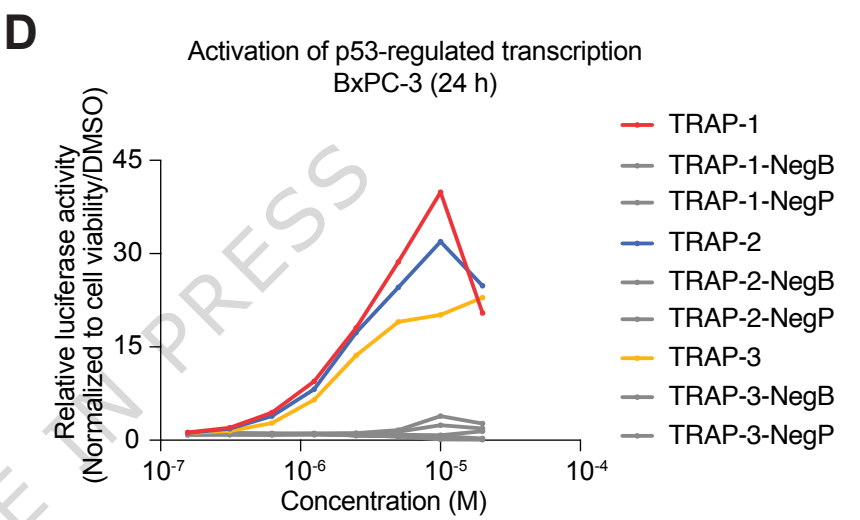

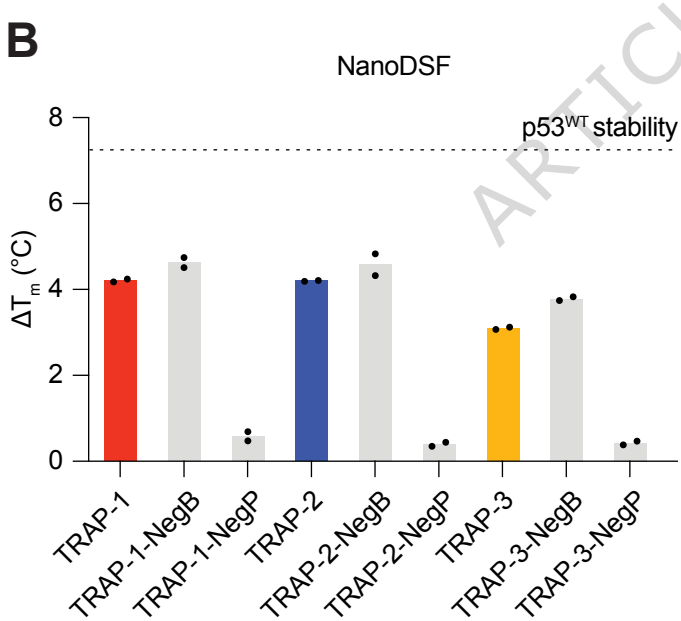

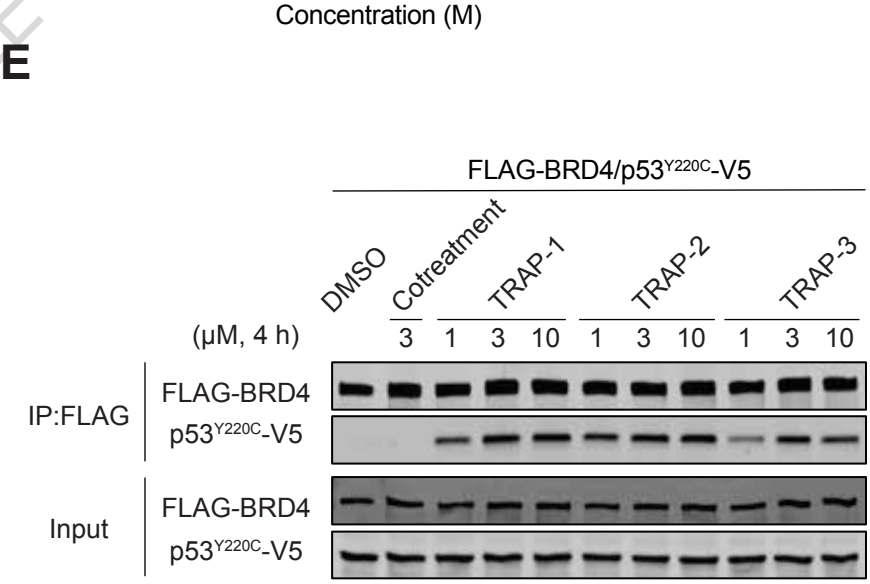

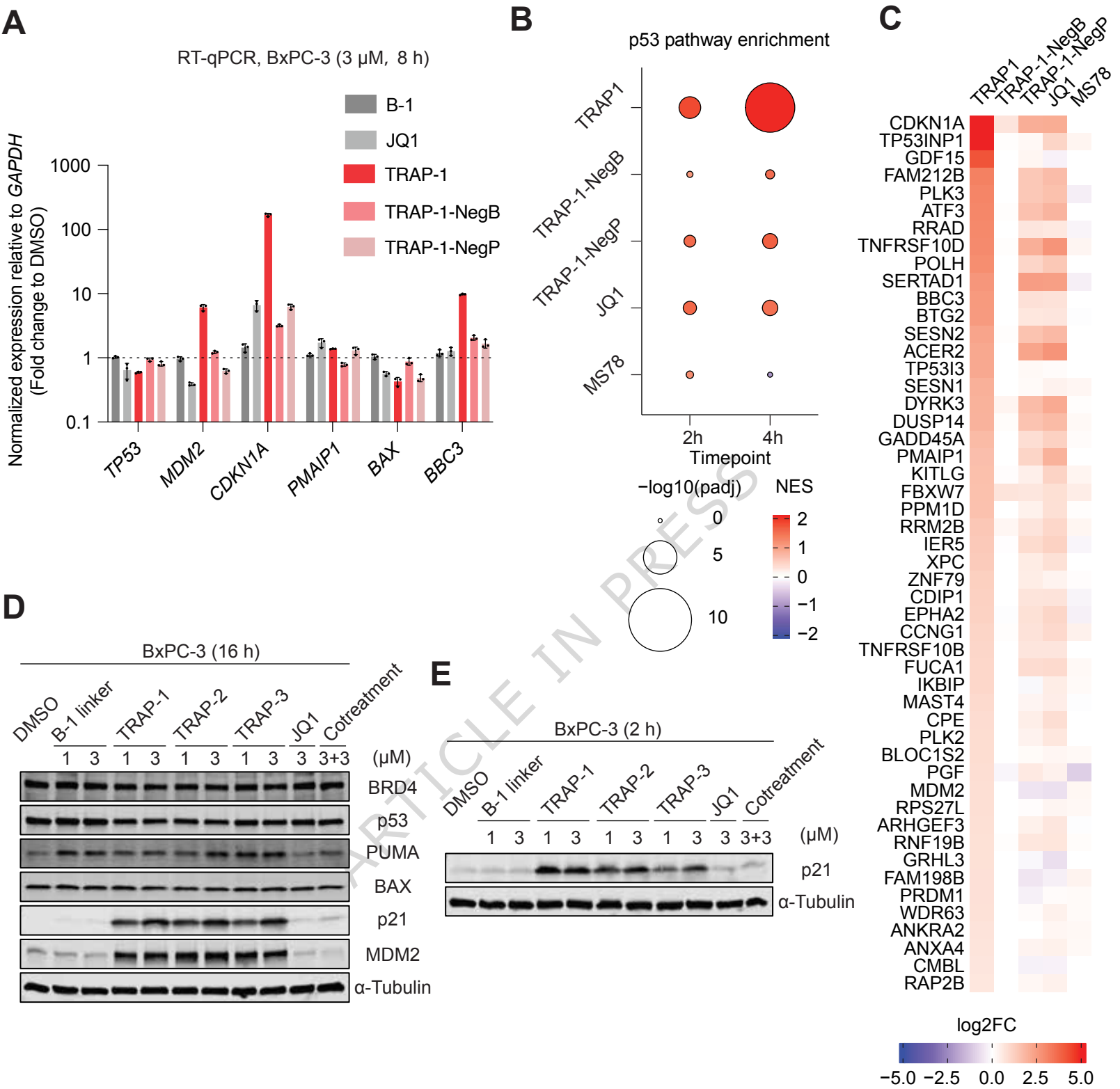

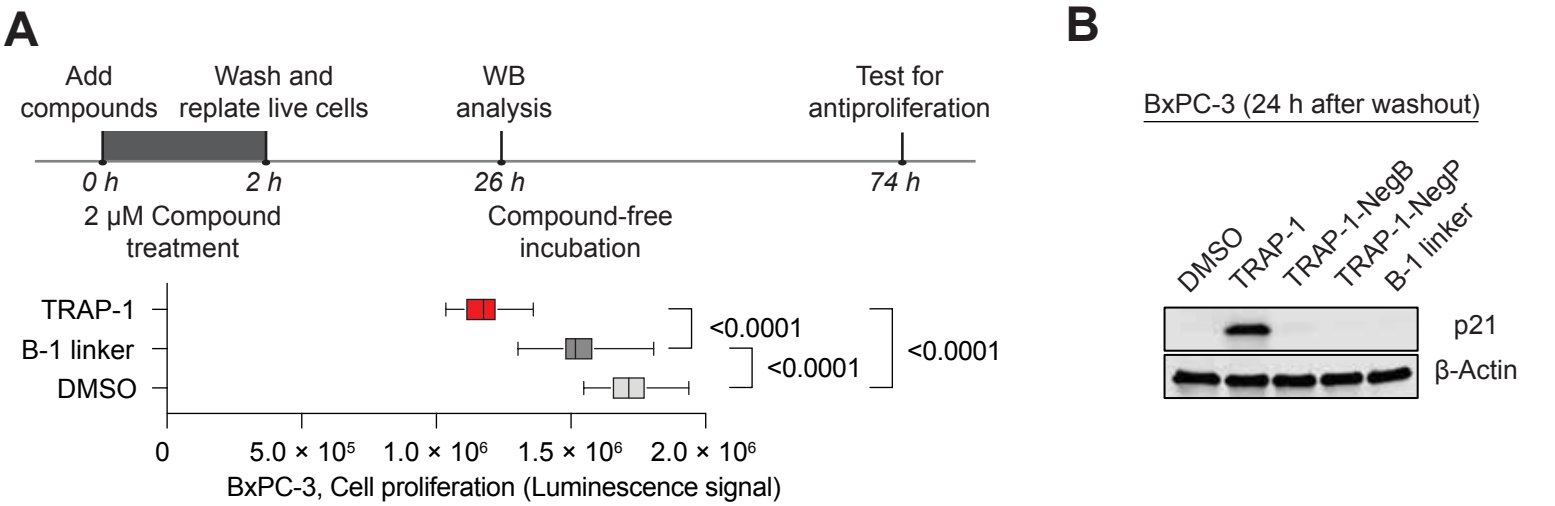
A
Add compounds
Wash and replate live cells
WB analysis
Test for antiproliferation
0 h
2 h
26 h
74 h
2 μM Compound treatment
Compound-free incubation
TRAP-1
B-1 linker
DMSO
<0.0001
<0.0001
<0.0001
0
5.0 × 10⁵
1.0 × 10⁶
1.5 × 10⁶
2.0 × 10⁶
BxPC-3, Cell proliferation (Luminescence signal)

B
BxPC-3 (24 h after washout)
DMSO
TRAP-1
TRAP-1-NegB
TRAP-1-NegP
B-1 linker
p21
β-Actin

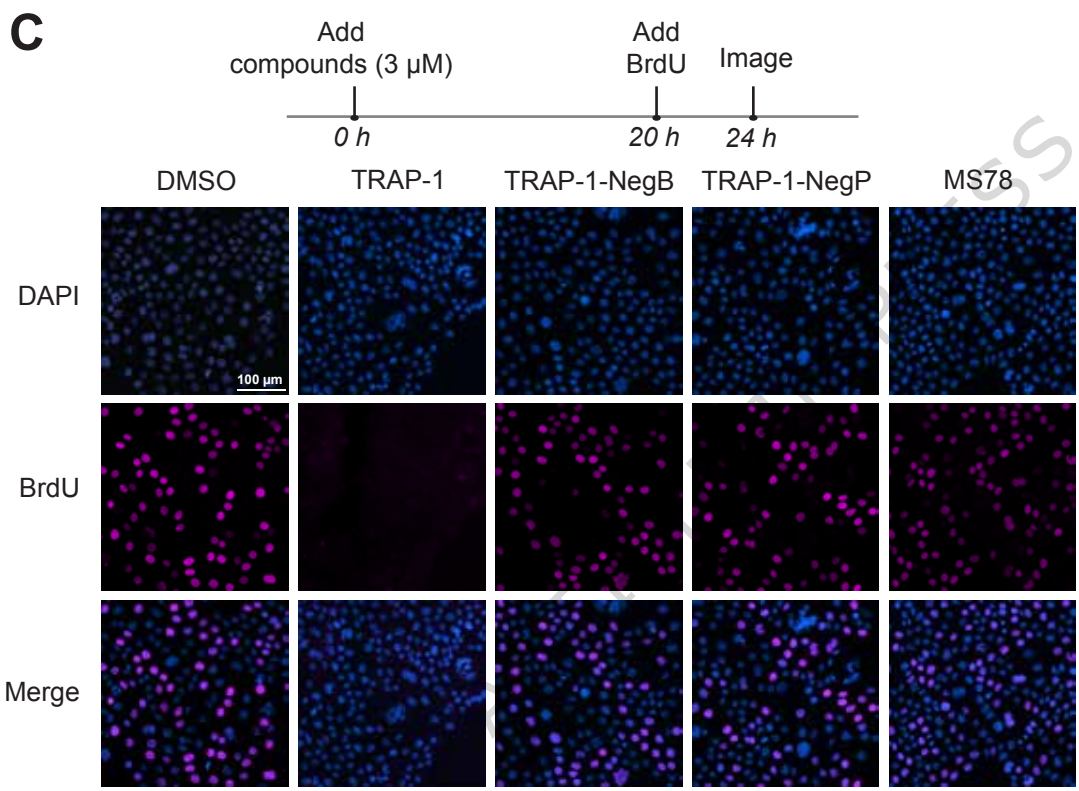
C
Add compounds (3 μM)
Add BrdU
Image
0 h
20 h
24 h
DMSO
TRAP-1
TRAP-1-NegB
TRAP-1-NegP
MS78
DAPI
BrdU
Merge
100 μm

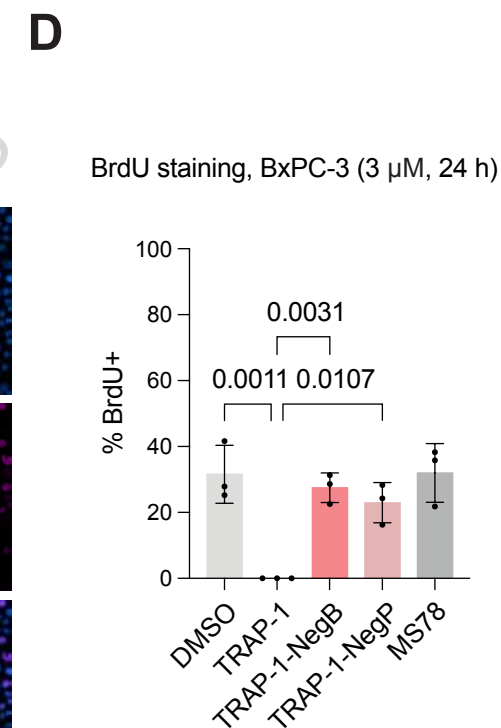
D
BrdU staining, BxPC-3 (3 μM, 24 h)
% BrdU+
100
80
60
40
20
0
0.0031
0.0011
0.0107
DMSO
TRAP-1
TRAP-1-NegB
TRAP-1-NegP
MS78

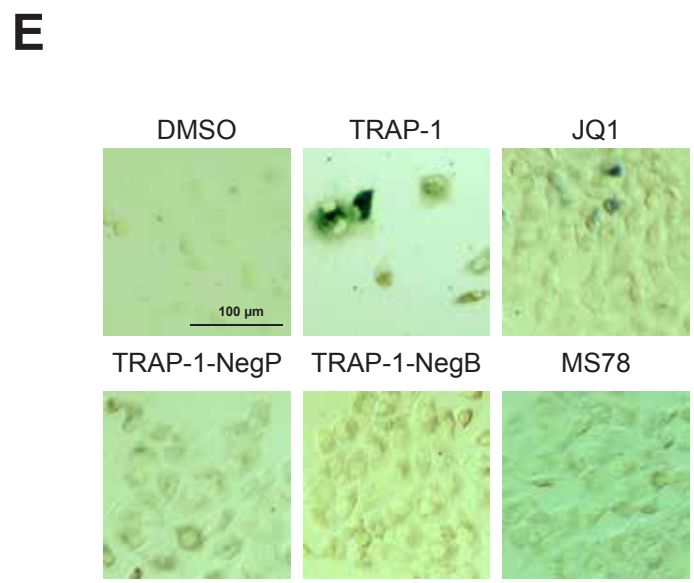
E
DMSO
TRAP-1
JQ1
TRAP-1-NegP
TRAP-1-NegB
MS78
100 μm

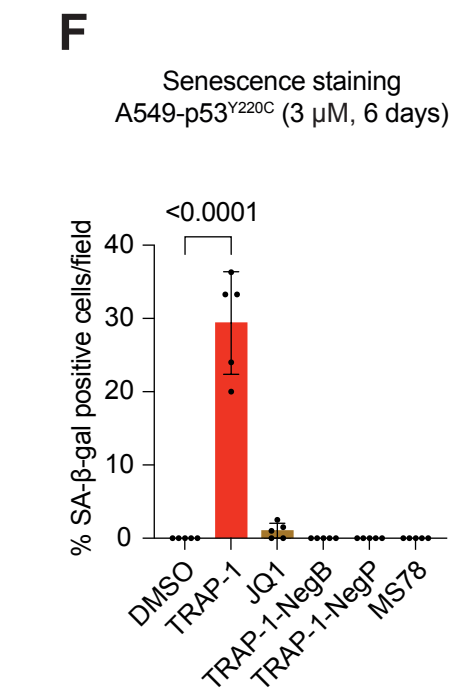
F
Senescence staining
A549-p53Y220C (3 μM, 6 days)
% SA-β-gal positive cells/field
40
30
20
10
0
<0.0001
DMSO
TRAP-1
JQ1
TRAP-1-NegB
TRAP-1-NegP
MS78

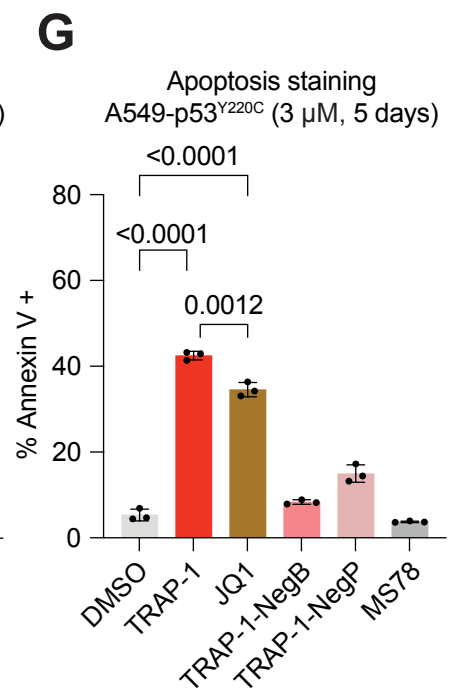
G
Apoptosis staining
A549-p53Y220C (3 μM, 5 days)
% Annexin V +
80
60
40
20
0
<0.0001
<0.0001
0.0012
DMSO
TRAP-1
JQ1
TRAP-1-NegB
TRAP-1-NegP
MS78

A

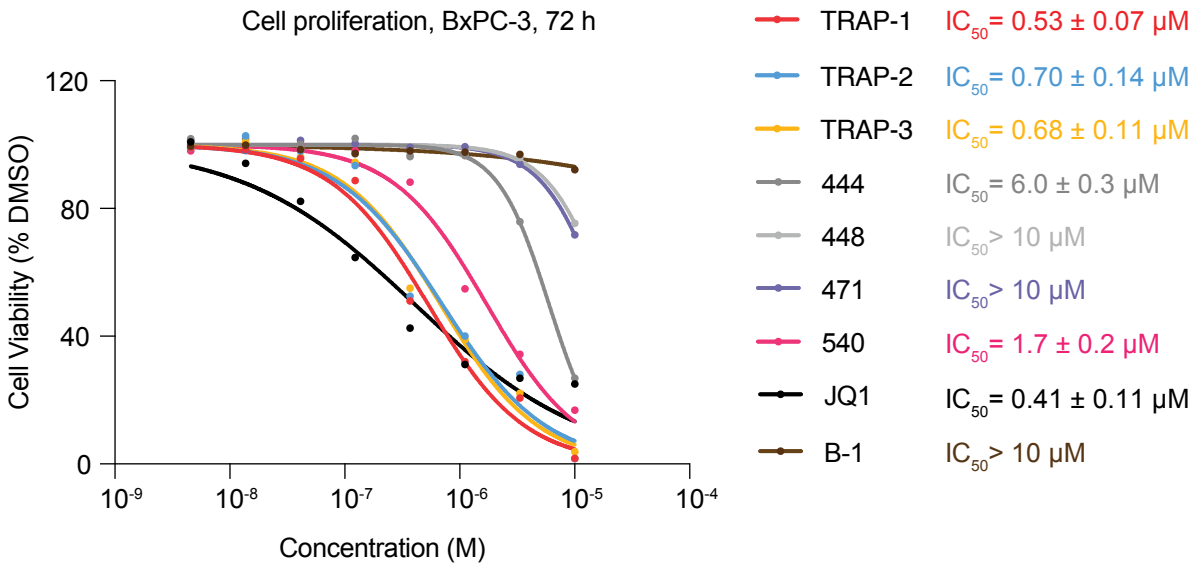
Cell proliferation, BxPC-3, 72 h
Cell Viability (% DMSO)
120
80
40
0
10-9
10-8
10-7
10-6
10-5
10-4
Concentration (M)
TRAP-1 IC50= 0.53 ± 0.07 µM
TRAP-2 IC50= 0.70 ± 0.14 µM
TRAP-3 IC50= 0.68 ± 0.11 µM
444 IC50= 6.0 ± 0.3 µM
448 IC50> 10 µM
471 IC50> 10 µM
540 IC50= 1.7 ± 0.2 µM
JQ1 IC50= 0.41 ± 0.11 µM
B-1 IC50> 10 µM

B

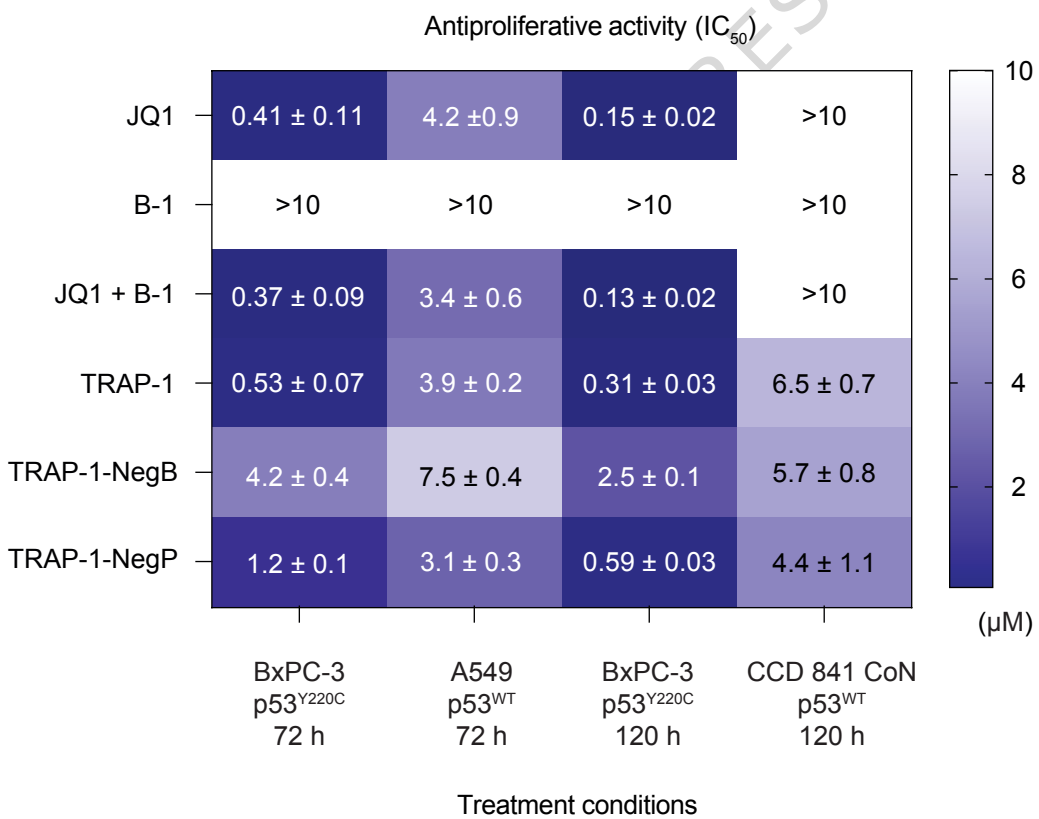
Antiproliferative activity (IC50)
JQ1
B-1
JQ1 + B-1
TRAP-1
TRAP-1-NegB
TRAP-1-NegP
0.41 ± 0.11
4.2 ±0.9
0.15 ± 0.02
>10
>10
>10
>10
>10
0.37 ± 0.09
3.4 ± 0.6
0.13 ± 0.02
>10
0.53 ± 0.07
3.9 ± 0.2
0.31 ± 0.03
6.5 ± 0.7
4.2 ± 0.4
7.5 ± 0.4
2.5 ± 0.1
5.7 ± 0.8
1.2 ± 0.1
3.1 ± 0.3
0.59 ± 0.03
4.4 ± 1.1
10
8
6
4
2
(µM)
BxPC-3 p53Y220C 72 h
A549 p53WT 72 h
BxPC-3 p53Y220C 120 h
CCD 841 CoN p53WT 120 h
Treatment conditions